

# **HYPERVIB IIa**

**A DETAILED NUMERICAL MODEL  
PROPOSED FOR FUTURE  
COMPUTER PROGRAM IMPLEMENTATION  
TO EVALUATE THE PENETRATION SPEED  
OF VIBRATORY DRIVEN SHEET PILES**

**BBRI**

**Dr. Alain E. Holeyman  
Irvine, September 1993**

## **CONTENTS**

### **MAIN TEXT**

1. INTRODUCTION
2. LOADING CONDITIONS
3. MODEL GEOMETRY
4. CONSTITUTIVE RELATIONSHIP
  - 4.1. Static stress-strain behavior
  - 4.2. Initial shear modulus and ultimate shear strength
  - 4.3. Secant shear modulus and hysteretic damping
  - 4.4. Strain rate effects
  - 4.5. Degradation law
  - 4.6. Soil liquefaction
  - 4.7. Generalized strain history
5. CPT EVALUATION OF PARAMETERS
6. BIBLIOGRAPHY

### **FIGURES**

### **COMPUTER DISKETTE**

## List of Figures

1. Model Geometry
2. Backbone Curve and Hysteretic Loop
3. In Situ Shear Modulus for saturated Clays (Seed and Idriss, 1970)
4. Moduli Determination for cohesionless Soils (seed and Idriss, 1970)
5. Typical Reduction of shear modulus with shear strain for saturated clays (Seed and Idriss, 1970)
6. Variation of shear modulus with shear strain for sands (Seed and Idriss, 1970)
7. Hyperbolic Law (Chart 5)
8. Damping Ratio (Dobry and Vucetic, 1987)
9. Modulus and Damping Curves (Vucetic and Dobry, 1991)
10. Comparison of Static and Dynamic tests Results (Dobry and Vucetic, 1987)
11. Sketch of the results and the definition of parameters of a cyclic strain controlled simple shear test on NC clay (Vucetic, 1993)
12. Degradation Index Versus number of cycles (Dobry and Vucetic, 1987)
13. Effect of the Plasticity Index on the degradation parameter (Vucetic, 1993)
14. Volume change of fully saturated sand in cyclic strain-controlled drained simple shear test (Youd, 1972)
15. Build up of residual pore pressure in different sands in undrained cyclic triaxial strain-controlled tests (Dobry, in NCR, 1985)
16. Schematic illustration of mechanism of pore pressure generation during cyclic loading (Seed and Idriss, 1982)
17. Tentative relationship between strength and SPT N-value (Seed, 1984)
18. Friction Ratio Correlations with fines content and PI (Chart 2)
19. Friction Modifier (Chart 3)
20. Effect of the plasticity on the cyclic threshold Shear Strain (Vucetic, 1993)

21. Threshold Shear strain (Chart 4)
22. Hyperbolic law to evaluate  $G/G_{max}$  and Relative Energy Loss (Chart 5)
23. Degradation Parameter Vs shear strain for different PI (Chart 6a)
24. Degradation Parameter Vs shear strain for different FR (Chart 6b)
25. Degradation Parameter Vs shear strain for different FR - Log scale(Chart 6c)
27. Degradation Parameter - high values - Vs shear strain for different FR (Chart 6d)
28. Degradation Parameter - high values - Vs shear strain for different FR (Chart 6e)
29. Degradation Vs Strain (FR=1%) - (Chart 10a)
30. Degradation Vs Strain (FR=2%) - (Chart 10b)
31. Degradation Vs Strain (FR=3%) - (Chart 10c)
32. Degradation Vs Strain (FR=4%) - (Chart 10d)
33. Pore pressure Vs damage parameter (Finn, 1981)
34. Pore pressure Vs damage parameter (Chart 7)
35. Pore pressure Vs cyclic shear Strain (Chart 8)
36. Pore pressure Vs relative strain for different numbers of cycles (Chart 9)

**NOTE:** Charts can be found in a digital form in the enclosed diskette (Excel file)

## 1. INTRODUCTION

This interim report presents the results of the fundamental development of a detailed model aimed at representing the dynamic response of soils under cyclic loading. The characterization of the soil model is provided herein as phase IIa of the Hypervib project. The model is to be incorporated into a numerical algorithm under phase IIb, such that numerical simulations can be produced with a single soil layer loaded by a rigid sheet pile actuated by a vibrator. Based on results of numerical simulations, the basic or refined soil model developed under phase II would be incorporated into a potentially more complex model simulating several soil layers and the elasticity of the sheet pile (Phase III). The numerical substantiation of the laws governing the soil behavior of the proposed model (Phase IIa) is provided on the enclosed computer diskette in the form of Excel spread sheets and charts.

## 2. LOADING CONDITIONS

The source of the cyclic loading acting upon the soil is a sheet pile being activated by a vibrator. The vibrations are essentially vertical and as a first approximation the vibration pattern of the surrounding soil can be considered to possess cylindrical symmetry. Although stresses are often used as the primary boundary condition in laboratory experiments, it is our opinion that in the case of a vibrating sheet pile, the governing boundary condition should be cinematic rather than dynamic: calculations performed with the phase I program show that the vibratory behavior (i.e. the amplitude of the movement) of the sheet pile itself is not strongly influenced by the soil resistance. In soft soils the shear stress resisting the sheet pile movement is small while it is higher in stiffer soils. It is therefore of interest to base the present soil model on strain-controlled cyclic shear tests rather than stress-controlled shear tests.

The sheet pile will be represented essentially by a rigid mass acted upon by the inertial effects of the vibrator eccentric masses, and deriving restraint from the dynamic reactions of the surrounding soil. The model used to represent the soil reactions is described below.

## 3. MODEL GEOMETRY

For the purpose of the present analysis, the soil reactions will be separated into the skin friction and the toe resistance. The toe resistance will be represented by a single degree of freedom (sdf), commonly utilized in wave equation calculations (Holeyman, 1984). Because of its preponderance in the study of vibration and penetration of sheet piles, the skin friction will be addressed by a more complex model that aims at encompassing the fundamental aspects of the vibratory behavior of the soil around the sheet pile.

The geometric shape of the soil model surrounding the sheet pile is proposed to have cylindrical symmetry, as shown in Fig. 1. It is a disk with a thickness that increases linearly with the radius. Normalized to the penetration depth of the sheet pile, it has a thickness provided by the following equation:

$$h = h_0 \cdot (1 + 0.03 \cdot (r - r_0)/r_0) \quad (1)$$

The increase of the disk thickness with the radial distance tends to simulate the geometrical damping provided by the half space of soil located below the toe of the sheet pile. The equivalent radius of the sheet pile is obtained from perimeter considerations:

$$r_0 = \text{perimeter} / 2 \pi \quad (2)$$

The outer boundary of the model is fixed for practical reasons based on a trade-off between calculation time and zone where the evaluation of the vibrations is of interest. An energy absorbing boundary condition limits the lateral extent of the model at a distance large enough to ensure that deformations stay within the elastic range and to avoid artificial energy reflections.

The system of cylindrical waves propagating within the geometric model will be calculated by discretizing the medium into concentric rings that possess individual masses and that transmit forces to their neighbors. The shear force-displacement relationship between successive rings is established based on the stress-strain relationship. Because of the complexity and multitude of factors affecting this relationship, it will be referred to as "constitutive relationship", or "constitutive laws governing shear stress-strain behavior". Movement of the rings is evaluated from the time integration of the laws of motion, and in particular from the acceleration resulting from the net unbalanced loads acting on a particular ring.

Masses of the rings are obtained using the following formula:

$$M_i = \rho \cdot \pi \cdot (r_{i+1}^2 - r_i^2) \cdot (h_{i+1} + h_i) / 2 \quad (3)$$

Inter-ring reactions are obtained using the following relationships:

$$T_i = 2 \cdot r_i \cdot h_i \cdot G' \cdot (u_{i+1} - u_i) \quad (4)$$

with  $G'$  representing the generalized secant shear modulus as discussed in Section 4.

Movement of the rings are evaluated using the following set of equations:

$$a_i = (T_{i+1} - T_i) / M_i \quad (5)$$

$$v_i(t+dt) = v_i(t) + a_i \cdot dt \quad (6)$$

$$u_i(t+dt) = u_i(t) + v_i(t+dt) \cdot dt + \frac{1}{2} a_i \cdot dt \quad (7)$$

#### 4. CONSTITUTIVE RELATIONSHIP

The constitutive relationship proposed for the representation of the large-strain, dynamic and cyclic shear stress-strain behavior of the medium surrounding the vibrating sheet pile will be described by several laws addressing the following elements:

- Static stress-strain law expressing nonlinear behavior under monotonic loading and hysteresis upon strain reversal
- Shear modulus at small strains and ultimate shear strength based on soil characterization: nature, void ratio, overconsolidation ratio; all of which should be correlated to  $q_c$  and FR obtained from CPT tests.
- Softening and increase of hysteretic damping with increasing strain based on soil characterization
- Effect of strain rate on initial shear modulus and ultimate strength
- Degradation of properties resulting from the application of numerous cycles
- Generation of excess pore pressure leading to liquefaction and substantial loss of resistance
- Accommodation of variable strain amplitude history

The following sections address these components of the constitutive relationship.

#### 4.1. Static Stress-strain behavior

A typical stress-strain law is represented in Fig. 2, which highlights the following fundamental parameters:

G <sub>max</sub> :	initial (or tangent) shear modulus
S <sub>max</sub> :	ultimate shear strength
G <sub>s</sub> :	secant (or equivalent) shear modulus
λ:	hysteretic (or intrinsic) damping ratio

Both G<sub>s</sub> and λ are strain-dependent parameters that need to be described by specific laws.

#### 4.2. Initial Shear modulus and ultimate shear strength

Numerous studies have dealt with the initial shear modulus to be used in earthquake engineering, and are summarized in Figs. 3 through 6. However, because most of them are supported by parameters determined in the laboratory we recommend an empirical approach based on correlations with CPT data, as discussed in Section 5:

$$G_{max} = K \cdot q_c \quad (8)$$

$$S_{max} = \text{Beta} \cdot f_s \quad (9)$$

#### 4.3. Secant Shear Modulus and Hysteretic Damping

As can be observed in Fig. 2, G<sub>s</sub> decreases with the shear strain during the initial monotonic loading. The curve that represents the initial monotonic loading is referred to as the initial "backbone" curve, because it also serves as the basis to generate the family of curves corresponding to unloading and reloading. A mathematical formulation due to Kondner (1963) is frequently employed to describe the initial backbone curve in earthquake engineering:

$$\eta = \tau / \tau_{max} = \delta / (\delta + 1) \quad \text{with} \quad \delta = \gamma / \gamma_r = \gamma \cdot G_{max} / \tau_{max} \quad (10)$$

It is of interest to show the hyperbolic law using reduced variables η, the mobilization ratio and δ, the relative shear, as shown in Fig. 7 (Chart 7). γ<sub>r</sub> is called the reference strain. Two of the parameters G<sub>max</sub>, γ<sub>r</sub>, and τ<sub>max</sub> are generally adjusted from laboratory experiments. In the case of CPT data, we propose to use the following values:

$$\tau_{max} = S_{max} \quad (11)$$

$$\gamma_r = S_{max} / G_{max}$$

From the point of maximum straining, the unloading curve is described by the following equation:

$$\tau - \tau_o = (\gamma - \gamma_o) / (1/G_{max} + (\gamma - \gamma_o) / 2\tau_{max}) \quad (12)$$

It can be observed that the unloading curve conforms to what are known as Masing's rules 1 and 2 (Masing, 1926):

Rule 1: The shear tangent modulus at each stress-strain reversal assumes a value equal to the initial tangent modulus of the backbone curve,  $G_{max}$ ,

Rule 2: Up to the point of intersection with the line described by the stress-strain curve of the previous cycle, the shape of the reloading curve of the subsequent cycle is the same as that of the backbone curve enlarged by a factor of two.

The energy contained in a loop depends for a given soil on the amplitude of the cyclic strain. Empirical data collected on the damping ratio is presented in Fig. 8 as a function of the cyclic shear strain  $\gamma_c$ . It can be noted that the damping ratio increases with  $\gamma_c$  as the soil undergoes higher plastic deformations.

We propose to utilize the unifying approach recently developed by Vucetic and Dobry (1991) to accommodate the influence of the nature of the material characterized in Fig. 9 by the plasticity index. The damping ratio obtained by integrating directly the area defined by a loop in the stress-strain diagram has been represented also in Fig. 5 to demonstrate the ability of the hyperbolic law in reproducing the experimental observation. The PI influencing the value of the reference strain  $\gamma_r$  will be correlated to the friction ratio as discussed in Section 5.

#### **4.4. Strain Rate Effects**

Although it is well known that undrained modulus and shear strength increase with increasing strain rate (see Fig. 10), experimental data generated under different apparatuses and loading conditions lead to different conclusions. Based on our review of the literature, it seems that a viscosity mechanism would provide a satisfactory framework for understanding the strain rate effect observed when comparing fast and slow undrained monotonic stress-strain curves, as well as for explaining the roundness of the loop tips during a sinusoidally strain-controlled cyclic test. Evidence would point to the fact that sands and non plastic silts have very small viscosity in that their stress-strain loops exhibit sharp rather than rounded tips.

The mathematical functions proposed in the literature to represent the nonlinear viscosity also depend on the observations. We propose to adopt a power law:

$$\tau_{dyn} = \tau_{stat} \cdot (1 + J \cdot \dot{\gamma}^n) \quad (13)$$

The advantage of that mathematical form is that resistance does not become zero at zero strain rate but that it takes orders of magnitude of variation in the strain rate to provide tangible increases in both the modulus and the ultimate strength. The J coefficient and n exponent depend on the nature of the soil. Based on pile driving data, we propose to use  $n=0.2$  and  $J=0.3 \text{ s}^{-0.2}$  for plastic soils. J should therefore essentially depend on the plasticity of the soil, and thus on the FR obtained from CPT tests.

#### **4.5. Degradation Law**

When subjected to undrained cyclic loading involving a number N of large strain cycles, the soil structure continuously deteriorates, the pore pressure increases, and the secant shear modulus decreases with N. This process is called cyclic stiffness degradation, and for the type of loading involved with the vibratory penetration of sheet piles, can be best characterized on the basis of strain controlled tests. Typical results of strain-controlled tests are provided in Fig. 11, where the degradation

is clearly expressed by the decrease of the amplitude of the peak stress mobilized at successive cycles.

The quantification of the degradation process call for the introduction of the degradation index  $\Delta$ , defined by:

$$\tau_n = \Delta \cdot \tau_1 \quad (14)$$

Laboratory results conducted at constant cyclic strain show that in many soils, the degradation index can be approximated by the relationship (see Fig. 12):

$$\Delta = N^{-t} \quad (15)$$

The exponent  $t$ , called degradation parameter, depends mainly on the amplitude of the cyclic strain and the nature of the material (PI), as indicated in Fig. 13 (Vucetic, 1993). It is noteworthy that the degradation parameter assumes a zero value at strains smaller than what is called the cyclic threshold shear strain,  $\gamma_{TV}$ . The threshold strain increases with the plasticity of the soil, as suggested in Fig. 13.

#### **4.6. Soil liquefaction**

For some time, it has been recognized by earthquake engineers that liquefaction of loose sandy soils was a major cause of potential damage during earthquake induced cyclic loading. In parallel, vibration induced compaction of saturated sands has received attention not only from the earthquake engineering community, but also from the vibro-compaction specialists. Recent advances tend to indicate that build up of pore pressures (eventually leading to liquefaction) and volume reduction of cyclically loaded materials are the expression of the same phenomenon, i.e. the irreversible tendency for a particulate arrangement to achieve a denser packing when sheared back and forth.

Under drained conditions, the volume reduction is immediate (see Fig. 14). Under undrained conditions, the tendency for volume reduction is expressed by an increase in the pore water pressure (see Fig. 15), such that the effective stress reduces to a value corresponding to equilibrium on the volumetric unloading curve, as shown in Fig. 16. It is then required to wait for the sample to consolidate in order to see the volume reduction take place. The Seed school of earthquake engineering endorses a stress driven evaluation of the liquefaction condition. Liquefaction occurs essentially when the excess pore pressure becomes equal to the total stress, at which point the effective stress has become zero, and the frictional component of the resistance vanishes. The medium behaves like a fluid, with a very low residual resistance, the value of which may be assessed using the concepts of critical state soil mechanics (Schoffield and Wroth, 1968). The residual strength of liquefied soil has been studied to evaluate the post-earthquake stability of slopes; Fig. 17 provides an indication of values recommended by Seed (1984).

Because the Seed approach to liquefaction evaluation is in great part founded on empirical observations and under the assumption of a plane strain horizontal cyclic shear stress loading (Seed and De Alba, 1986), we consider it perilous to apply it to a situation where the shear is applied along vertical cylinders. By contrast, the Dobry school of earthquake engineering, which endorses a strain driven evaluation of the build up of pore pressure allows a more direct, and therefore more reliable, transposition to the problem of the vibrations induced by a vertically vibrating sheet pile.

Most importantly, it would appear that the void ratio change resulting from cyclic loading is more uniquely related to a cyclic strain history than to a cyclic stress history, as evidenced in the early tests conducted on drained sands by Youd (1972). In addition, this framework of analysis enables the

threshold cyclic strain to encompass in a single concept the intrinsic relationship between degradation and pore pressure build-up, with the advantage that it can be applied to general categories of soils (sands to clays).

#### **4.7. Generalized strain history**

Because the constitutive relationships parameters are generally established on the basis of constant strain, laboratory controlled tests, it is necessary to formulate a means to follow the dynamic behavior of the medium under the non regular types of loading present during the vibro-penetration of a sheet pile: start-up and turn-off, progressive modification of soil properties resulting from degradation, etc. We will therefore introduce two additional Masing rules to accommodate non-repetitive straining paths:

Rule 3: If the reloading stress-strain curve intersects the backbone curve, it subsequently follows the path described by this backbone curve, and

Rule 4: If the current reloading (unloading) curve intersects the line described by the previous reloading (unloading) curve, by approaching it from within the loop, the new curve will follow this path described by the previous curve.

Degradation can also be represented under irregular loading, provided that a degraded backbone curve is used instead of the initial backbone curve. The degraded backbone curve is completely defined by the degradation index  $\Delta$ , the equivalent value of which must be ascertained based on the amplitude and number of previous straining cycles. This will require to update the current degradation index using the following equations:

$$N_{eq} = \Delta^{(-1/t)} \quad (16)$$

$$\Delta = (N_{eq} + 1)^{-t} \quad (17)$$

## **5. CPT EVALUATION OF PARAMETERS**

The CPT has been chosen as the basic sounding upon which the evaluation of the vibro-penetration of sheet piles is to be conducted. It provides simple, yet ad hoc parameters that can be related directly or indirectly to the parameters necessary to model the soil behavior. This section summarizes the proposed approach; to be refined based on full scale tests to be conducted by the BBRI.

### ***PI***

Because an number of constitutive laws call for a value of the plasticity index to account for the fineness and activity of the soil, a basic correlation is proposed to relate PI to the friction ratio. It is generally accepted that the friction ratio as obtained from the electric CPT test is a significant index that allows the categorization of soil types. Several empirical correlations have been established between friction ratio (FR) and fines contents (<16  $\mu\text{m}$  per Begemann, 1965 and <74  $\mu\text{m}$  per ASTM classification). Table 1 summarizes deductions made from the synthesis of different soil classification systems; results are presented graphically in Fig. 18 (Chart 2).

Based on these comparisons, we propose the following correlation:

$$PI = 50 \cdot (1 + \tanh (FR - 3.5\%)) \quad (18)$$

formula which is also represented in Fig. 18 to confirm its relevance.

**G<sub>max</sub>**

$$G_{max} = K \cdot q_c \quad (19)$$

$$\text{with } K=15 \quad (20)$$

**S<sub>max</sub>**

$$S_{max} = \text{Beta} \cdot fs \quad (21)$$

to account for limited displacement induced by sheet pile with Beta, friction modifier shown in Fig. 19 (Chart 3) and given by:

$$\text{Beta} = 0.65 + 0.35 \cdot \tanh 1.5(FR-3.5\%) \quad (22)$$

**γ<sub>r</sub>**

$$\gamma_r = S_{max}/G_{max} = \text{Beta} \cdot fs / (15 q_c) \quad , \text{ per (19), (20), and (21)} \quad (23)$$

$$= \text{Beta} \cdot FR / 15 \quad (24)$$

$$= 2 \gamma_{\tau U} \quad (24)$$

**γ<sub>τU</sub>**

$$\gamma_{\tau U} = \text{Beta} \cdot FR / 30 \quad (25)$$

Compare Fig. 19 (Chart 4) and 20 (experimental data) to observe good agreement of proposed correlations

**G**

G given by hyperbolic law (equation (10))

See Fig. 22 (Chart 5)

**t**

$$t = (\gamma/\gamma_{\tau U} - 1)^{1/2} / (PI/2 + 25) \quad (26)$$

Compare Fig. 23 (Chart 6a) to Fig. 13 (experimental data) to observe good correlation based on PI

See Figs. 24 through 28 for degradation parameter t based on FR

**Δ**

$$\Delta = N^{-t} \quad (27)$$

See Figs. 29 through 32 for estimated degradation for different friction ratios

### **Pore Pressure Generation**

$$du/\sigma' = \frac{1}{4} (\text{Rel. En. Loss}) \cdot \ln(1 + \frac{1}{2} \kappa) \quad (28)$$

See Fig. 22 (Chart 5) for Relative Energy Loss

$\kappa$  = damage parameter (Finn, 1981), given by:

$$\kappa = \xi e^{\lambda \gamma} \quad (29)$$

$\xi$  = length of strain path

=  $4 N \gamma$ , for constant amplitude cycles

$\lambda = 5$ , per Fig. 33

See Fig. 34 (Chart 7) for conformance of equation (29)

Compare Fig. 35 (chart 8) to Fig. 15 for agreement

See Fig. 36 for influence of N on pore pressure buildup

### **qptmax**

$$q_{ptmax} = q_c / 1.3 \quad (30)$$

to account for 2-D failure mechanism

### **J**

$$J = 0.10 FR \quad (31)$$

## **6. BIBLIOGRAPHY**

- Andersen, K.H., Pool, J.H., Brown, S.F. and Rosenbrand, W.F. (1980). "Cyclic and Static Laboratory Tests on Drammen Clay." *Journal of the Geotechnical Engineering Division*, Proc. ASCE, Vol. 106, No. GT5, pp. 499-529.
- Andersen, K.H. (1983). "Strength and Deformation Properties of Clay Subjected to Cyclic Loading." Report No. 52412-8, Norwegian Geotechnical Institute, Oslo, Norway.
- Anderson, D.G. and Richart, Jr., F.E. (1976). "Effects of Straining on Shear Modulus of Clays." *Journal of the Geotechnical Engineering Division*, Vol. 102, No. GT9, pp. 975-987.
- Andreasson B.A. (1979). "Deformation Characteristics of Soft, High-Plastic Clays under Dynamic Loading Conditions." Ph.D. Thesis, Dept. of Geotechnical Engineering, Chalmers University of Technology, Gothenburg, Sweden.
- Andreasson, B.A. (1981). "Dynamic Deformation Characteristics of a Soft Clay." International Conference on Recent Advances in Geotechnical Earthquake Engineering and Soil Dynamics, St. Louis, Missouri. Vol. I, pp. 65-70.
- A.S.T.M. D 2487 -90 (1990). "Standard Test Method for Classification of Soils for Engineering Purposes.", 1991 Annual Book of ASTM Standards, Vol 04.08, pp 309-319.
- Begemann, H. K. S. (1965). "The Friction Jacket Cone as an Aid in Determining the Soil Profile." Proc. Vth ICSMFE, Montreal, Vol 1.

- Castro, G. and Poulos, S.J. (1977) "Factors affecting Liquefaction and Cyclic Mobility," *Journal of the Soil Mechanics and Foundations Division*, ASCE Vol.103, No SM6, June, pp. 501-506.
- Chu, H.H. and Vucetic, M. (1992). "Settlement of Compacted Clay in a Cyclic Direct Simple Shear Device." *ASTM Geotechnical Testing Journal*, Vol. 15, No. 4, pp. 371-379.
- Deresiewicz, H. (1973). "Bodies in Contact with Applications to Granular Media," included in *RD. Mindlin and Applied Mechanics*, G. Herrman, Editor, Pergamon Press, NY.
- Dobry, R., Ladd, R.S., Yokel, F.Y., Chung, R.M., and Powell, D. (1982). "Prediction of Pore Water Pressure Buildup and Liquefaction of Sands During Earthquakes by the Cyclic Strain Method." National Bureau of Standards Building Science Series 138, July 1982, 150 pp.
- Dobry, R., Yokel, F. and Add, R'S, (1981), "Liquefaction Potential of Overconsolidated Sands in Moderately Seismic Areas." *Proceedings of the Conference on Earthquakes and Earthquake Engineering in the Eastern U.S.*, Knoxville, TN, Sept., Vol. 2. pp. 643-664.
- Dobry R. (1991). "Soil Properties and Earthquake Ground Response." *Guest Lecture, Proceedings, Tenth European Conference on Soil Mechanics and Foundation Engineering*, Florence, Italy, Vol. 4.
- Dobry, R. and Ladd, R (1980). Discussion of "Soil Liquefaction and Cyclic Mobility Evaluation for Level Ground During Earthquakes" by H B. Seed and "Liquefaction Potential: Science versus Practice," by R B. Peck, *Journal of the Geotechnical Engineering Division*, ASCE, Vol. 106, GT. 6, June, pp. 720-724.
- Dobry, R. and Ng, T.-T. (1989). "Discrete Modelling of Stress-Strain Behavior of Granular Media at Small and Large Strains." *In DEM 1st U.S. Conference on discrete Element Methods*, G.G.W. Mustoe, M. Henriksen, and H.-P. Huttelmaier, Editors, CSM Press, Golden, CO.
- Dobry, R. and Swiger, W.F. (1979). "Threshold Strain and Cyclic Behavior of Cohesionless Soils. " *Proc. 3rd ASCE/EMDE Specialty Conference*. Austin, Texas, pp. 521-525.
- Dobry, R. and Vucetic, M. (1987). "State-of-the-Art Report: Dynamic Properties and Response of Soft Clay Deposits. " *Proceedings of the Intl. Symposium on Geotechnical Eng. of Soft Soils*, Mexico City, Vol. 2, pp. 51-87.
- Drnevich, V.P., Hall, J.R., Jr., and Richart, F.E., Jr. (1967). "Effects of Amplitude of Vibration on the Shear Modulus of Sand." *Proceedings of the International Symposium on Wave Propagation and Dynamic Properties of Earth Materials*, Albuquerque, N.M., pp. 189-199.
- Drnevich, V.P. and Richart, F.E., Jr. (1970). "Dynamic Prestraining of Dry Sand." *Journal of the Soil Mechanics and Foundations Division*, ASCE Vol.96, No SM2, Proc. Paper 7160, march, pp. 453-469.
- Dyvik, R., Dobry, R., Thomas, G.E. and Pierce, W.G. (1984). "Influence of Consolidation Shear Stresses and Relative Density on Threshold Strain and Pore Pressure During Cyclic Straining of Saturated Sands," Miscellaneous Paper GL-84-15, Department of the Army, UPS. Army Corps of Engineers, Washington, D.C.

- Finn, W. D. L. (1981) "Liquefaction Potential: Developments Since 1976", *Proceedings, Intl. Conf. on Recent Advances in Geotechnical Earthquake Engineering and Soil Dynamics*, St. Louis, Missouri, Vol. II, pp.655-681.
- Georgiannou, V.N., Rampello, S. and Silvestri F. (1991). "Static and Dynamic Measurements of Undrained Stiffness of Natural Overconsolidated Clays." *Proceedings, 10th European Conference on Soil Mechanics and Foundation*, Florence, Italy, Vol. 1, pp. 91-95.
- Hardin, B.O. and Black, W.L. (1968). "Vibration Modulus of Normally Consolidated Clay." *Journal of the Soil Mechanics and Foundations Division*, ASCE, Vol. 94, No. SM2, Proc. Paper 5833, pp. 353-369.
- Holeyman, A. (1992) "Technology of Pile Dynamic Testing," Keynote Lecture, *Proceedings of the Fourth International Conference on the Application of Stress-Wave Theory to Piles*, The Hague, September 21-24, 1992, 21p.
- Holeyman, A. (1990) "Pile Dynamic Testing - European Experience," presentation at the ASCE Los Angeles Section meeting of January 1990, 12 p. (handout).
- Prakash, S., and Holeyman, A. (1988) ", General Report on Discussion Session 15 - Static and Dynamic Testing of Piles," *Proceedings of the XIIth ICSMFE*, Rio de Janeiro, August 1989, Vol. 4, pp 2607 - 2616.
- Holeyman, A. , et al., (1988) " Comparative Dynamic Pile Testing in Belgium," *Proceedings of the 3rd International Conference on the Application of Stress-Wave Theory to Piles*, Ottawa, May 1988, pp. 542-554.
- Holeyman, A. (1988) "Modelling of Pile Dynamic Behavior at the Pile Base during Driving," *Proceedings of the 3rd International Conference on the Application of Stress-Wave Theory to Piles*, Ottawa, May 1988, pp. 174-185.
- Holeyman, A. (1987) "Etat de la Question sur les Essais de Mise en Charge Dynamique de Pieux," *Proceedings of the Belgian Symposium on Pile Dynamic Testing*, Brussels, November 1987, pp. II-50, II-103.
- Holeyman, A. (1985) "Influence of Soil Conditions on the Possibility of Pile Driving and Maximum Depth of Penetration," Chairman report on session 2, *Proceedings of the International Symposium on Penetrability and Drivability of Piles*, San Francisco, 10 August 1985, Vol. 2, pp. 16-22.
- Holeyman, A. (1985) "Static Versus Dynamic pile bearing capacity, Discussion to session 4," *Proceedings of the International Symposium on Penetrability and Drivability of Piles*, San Francisco, 10 August 1985, Vol. 2, pp. 80-82.
- Holeyman, A. (1985) "Dynamic non-linear skin friction of piles," *Proceedings of the International Symposium on Penetrability and Drivability of Piles*, San Francisco, 10 August 1985, Vol. 1, pp. 173-176.
- Holeyman, A. (1985) "Unidimensional modellization of dynamic footing behaviour," *Proceedings of the XIth I.C.S.M.F.E.*, San Francisco, 12-16 August, 1985, pp. 761-765.

- Holeyman, A. (1984) "Friction Behaviour of Piles During Driving," *Symposium on Geotechnical Aspects of Mass and Material Transportation*, December 3-7, 1984, AIT, Bangkok, pp. 34-56.
- Holeyman, A. (1984) "Contribution à l'étude du comportement transitoire non-linéaire des pieux pendant leur battage." Thèse présentée en vue de l'obtention du grade légal de Docteur en Sciences appliquées, Université Libre de Bruxelles, April, 1984, 584 pages.
- Idriss, I.M., Dobry, R, and Singh. R.D. (1978). "Nonlinear Behavior of Soft Clays during Cyclic Loading." *J. Geotechnical Engineering Div.*, ASCE, 104(GT12), pp. 1427- 1447.
- Ishihara, K. (1981). "Strength of Cohesive Soils Under Transient and Cyclic Loading Conditions. " State-of-the-Art in Earthquake Engineering, *Proceedings, Seventh World Conference on Earthquake Engineering*. Istanbul. Turkey. pp. 154-169.
- Ishihara, K. (1986). "Evaluation of Soil Properties for use in Earthquake Response Analysis," *Geomechanical Modelling in Engineering Practice*. R Dungar and J. A. Studer. eds.. A. Balkema, Rotterdam, the Netherlands, pp. 241-275
- Kondner, R. L., (1963). "Hyperbolic Stress-Strain Response: Cohesive Soils." *Journal of the Soil Mechanics and Foundations Division*, ASCE, Vol. 89, No. SM1, pp. 115-143, Jan.
- Ladd, R.S. (1982). "Geotechnical Laboratory Testing Program for Study and Evaluation of Liquefaction Ground Failure Using Stress and Strain Approaches: Heber Road site, October 13, 1979 Imperial Valley Earthquake," Vol. I to III, Woodward-Clyde Consultants, Eastern Region, Wayne, New Jersey.
- Ladd, R.S., Dobry, R., Dutko, P., Yokel, F.Y., and Chung, R.M. (1989). "Pore-Water Pressure Buildup in Clean Sands Because of Cyclic Straining." *Geotechnical Testing Journal*, GTJODJ, Vol. 12, No. 1, pp. 77-86.
- Macky, T.A. and Saada, A.S. (1984). "Dynamics of Anisotropic Clays under Large Strains." *Journal of the Geotechnical Engineering Division*, ASCE, Vol. 110, No. 4, pp. 487-504.
- Masing, G. (1926), "Eigenspannungen und Verfeistigung beim Messing", *Proceedings of Second International Congress of Applied Mechanics*, pp. 332-335.
- Matasovic, J. and Vucetic, M. (1993) "Analysis of Seismic Records Obtained on November 24, 1987, at the Wildlife Liquefaction Array." Research Report, Civil Eng. Dept., Univ. of California, Los Angeles.
- Matasovic, N. and Vucetic, M. (1992). "A Pore Pressure Model for Cyclic Straining of Clay." *Soils and Foundations*, Vol. 32, No. 3, pp. 156- 173.
- Matsuda, H. and Ohara, S. (1989). "Threshold Strain of Clay for Pore Pressure Buildup." *Proceedings, XII Intl. Conf. Soil Mechanics and Foundation Engineering*, Rio de Janeiro, Brazil, Earthquake Geotechnical Engineering Volume. pp. 127-130.
- Matsui, T., Ohara, H., and Ito, T. (1980). "Cyclic Stress-Strain History and Shear Characteristics of Clay." *Journal of the Geotechnical Engineering Division*, Proc. ASCE, Vol. 106, No. GT10, pp. 1101-1120.
- Mitchell, J.K (1976). *Fundamentals of Soil Behavior*. John Wiley & Sons, New York.

- NRC (1985). "Liquefaction of Soils During Earthquakes." National Research Council Committee on Earthquake Engineering, Report No. CETS-EE-001, Washington, D.C.
- Ohara, S. and Matsuda, H. (1988). "Study on Settlement of Saturated Clay Layer Induced by Cyclic Shear." *Soils and Foundation*, Proc. JSSMFE. Vol. 28. No. 3. pp. 103-113.
- Pyke, R.M. (1973). "Settlement and Liquefaction of Sands Under Multi-Directional Loading," Ph.D. thesis, University of California at Berkeley.
- Pyke, R., Seed, H.B., and Chen, C.K. (1975). "Settlement of Sands Under Multi-Directional Shaking." *Journal of the Geotechnical Engineering Division*, Proc. ASCE, Vol 101, No GT4, pp. 379-398.
- Schoffield, A., N., and Wroth, C., P., (1968). "Critical State Soil Mechanics", Mc Graw Hill Publishing Company Ltd., London.
- Seed, H.B. and Idriss, I.M. (1970). "Soil Moduli and Damping Factors for Dynamic Response Analyses." Earthquake Engineering Research Center, College of Engineering, University of California, Berkeley, Report No. EERC 70-10.
- Seed, H.B. and De Alba, P. (1986) "Use of SPT and CPT Tests for Evaluating the Liquefaction Resistance of Sands" *Proc. INSITU 86*, VA, 22p.
- Silver, M.L. and Seed, HUB. (1971). "Volume Changes in Sands During Cyclic Loading." *Journal of the Soil Mechanics and Foundations Division*, Proc. ASCE, Vol. 97, No. SM9, pp. 1171-1182.
- Stokoe, K.H. and Lodde, P.F. (1978). "Dynamic Response of San Francisco Bay Mud." *Earthquake Engineering and Soil Dynamics*, Vol. 2, ASCE, pp. 940-957.
- Stoll, R.D. and Kald. L. (1977). "Threshold of Dilation Under Cyclic Loading." Technical Note, *Journal of the Geotechnical Engineering Division*, Proc. ASCE, Vol. 103, No. GT10, pp 1174- 1178.
- Tan, K. and Vucetic, M. (1989). "Behavior of Medium and Low Plasticity Clays under Cyclic Simple Shear Conditions." *Proceedings of the 4th International Conference on Soil Dynamics and Earthquake Engineering*, Soil Dynamics and Liquefaction Volume, Mexico City, pp. 131-142.
- Tokimatsu, K. and Yoshimi, Y. (1983) "Empirical Correlation of Soil Liquefaction Based on SPT-Value and Fines contents," *Soils and Foundations*, Vol. 23, No. 4, December, pp. 56-74.
- Vucetic, M., Dobry, R., Petrakis, E., and Thomas, G.E. (1985). "Cyclic Simple Shear Behavior of Overconsolidated Offshore Clay." *Proceedings, Second International Conference on Soil Dynamics and Earthquake Engineering*, on board the Liner Queen Elizabeth 2, New York to Southampton, pp. 2- 107 to 2- 116.
- Vucetic, M. (1988). "Normalized Behavior of Offshore Clay Under Uniform Cyclic Loading." *Canadian Geotechnical Journal*, Vol 25, No. 1. pp. 33-41.
- Vucetic, M. (1991). General Report: "Model Testing in Cyclic Loading." *Proceedings of the Second International Conference on Recent Advances in Geotechnical Earthquake Engineering and Soil Dynamics*, St. Louis. Missouri. Vol. m, pp. 1985- 1990.

- Vucetic, M. (1992). "Soil Properties and Seismic Response." *Proceedings of the Tenth World Conference on Earthquake Engineering*, Madrid, Spain. A.A. Balkema, Vol. III. July, pp. 1199-1204.
- Vucetic, M. (1993). "Cyclic Threshold Shear Strains of Sands and Clays", UCLA Dept. of Civil Engineering, May 1993 - Personal Communication
- Vucetic, M. and Dobry, R. (1988). "Degradation of Marine Clays Under Cyclic Loading. *ASCE Journal of Geotechnical Engineering*, Vol. 114, No.2, pp.133-149.
- Vucetic, M. and Dobry, R. (1991). "Effect of Soil Plasticity on Cyclic Response." *ASCE Journal of Geotechnical Engineering*, Vol. 117, No. 1, pp. 89- 107.
- Watabe, M., et at. (1991). "Large Scale Field Tests on Quaternary Sand and Gravel Deposits for Seismic Siting Technology." *Proceedings, Second Intl. Conf. on Recent Advances in Geotechnical Earthquake Engineering and soil Dynamics*, St. Louis, Missouri, Vol. I, pp.271 -290.
- Youd, L.T. (1972). "Compaction of Sands by Repeated Shear Straining." *Journal of the Soil Mechanics and Foundations Division*, Proc. ASCE, Vol. 98, No. SM7, pp. 709-725.

**Table 1. CPT Friction Ratio Correlations**

<b>Soil Type</b>	Medium coarse sand	Medium sand	Fine sand	silty sand	clayey sand	sandy clay or loam	plastic silt	silty clay	clay
<b>Electrical cone friction ratio (FR )</b>	0.6 %	0.8 %	1.1 %	1.4 %	1.8 %	2.2 %	2.5 %	2.9 %	3.3 %
<b>Begemann &lt;16<math>\mu</math> fraction</b>	0 %	0 %	0 %	15 %	35 %	50 %	60 %	70 %	80 %
<b>ASTM Symbol</b>	SW SP	SW SP	SW SP	SM	SC	ML	CL	MH	CH
<b>% Fines (&lt;74<math>\mu</math>)</b>	< 5 %	< 5 %	< 5 %	12 - 50 %	12 - 50 %	> 50 %	> 50 %	> 50 %	> 50 %
<b>Plasticity properties</b>	NP	NP	NP	Below "A" line	Above "A" line	LL < 50 PI < 4 Below "A"	LL < 50 PI > 7 Above "A"	LL > 50 Below "A"	LL > 50 Above "A"

## FIGURES

## FIGURES

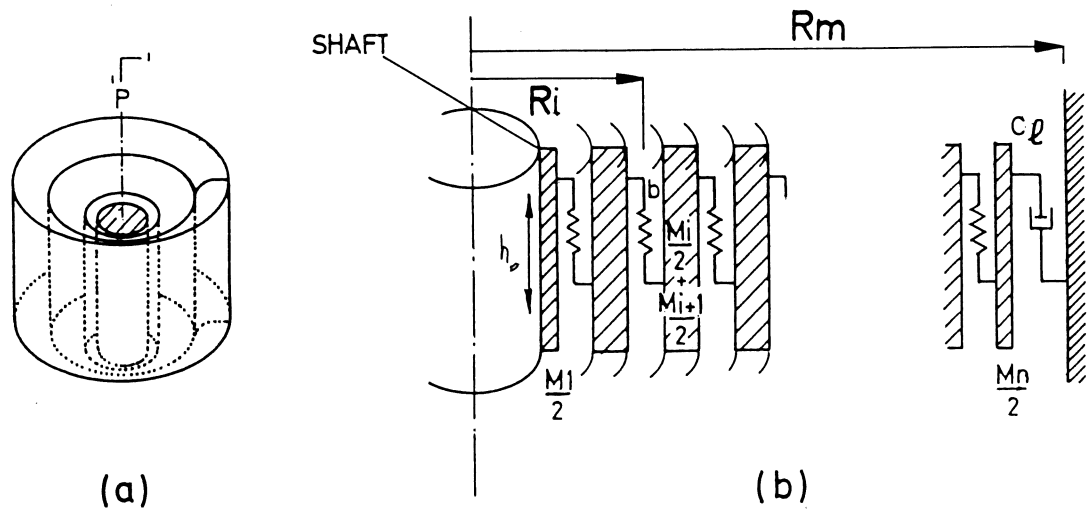
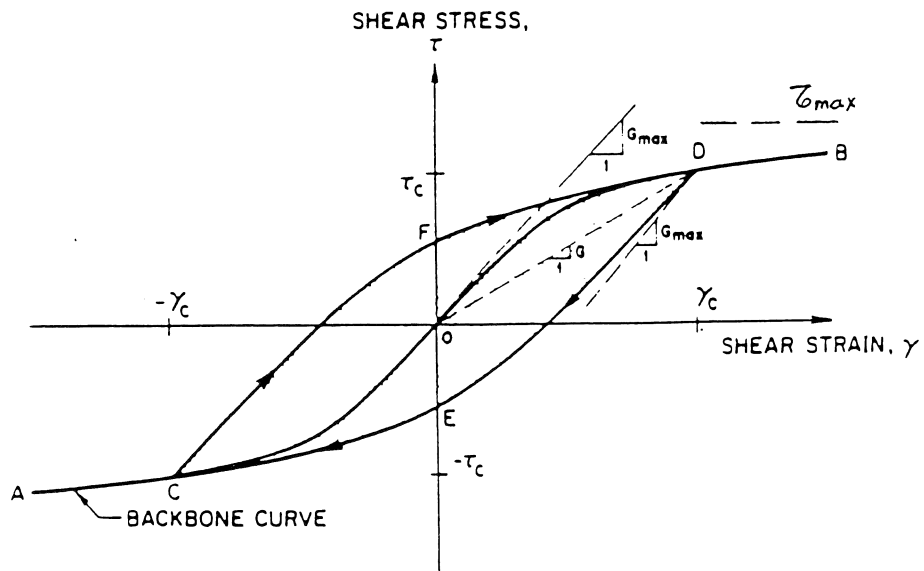


Fig. 1. Model Geometry



$G_{max}$  = Shear Modulus  $G$  at Very Small Strains  
 $= \rho \cdot V_s^2$   
 $V_s$  = Shear Wave Velocity  
 $\rho$  = Mass Density

Fig. 2. Backbone Curve and Hysteretic Loop.

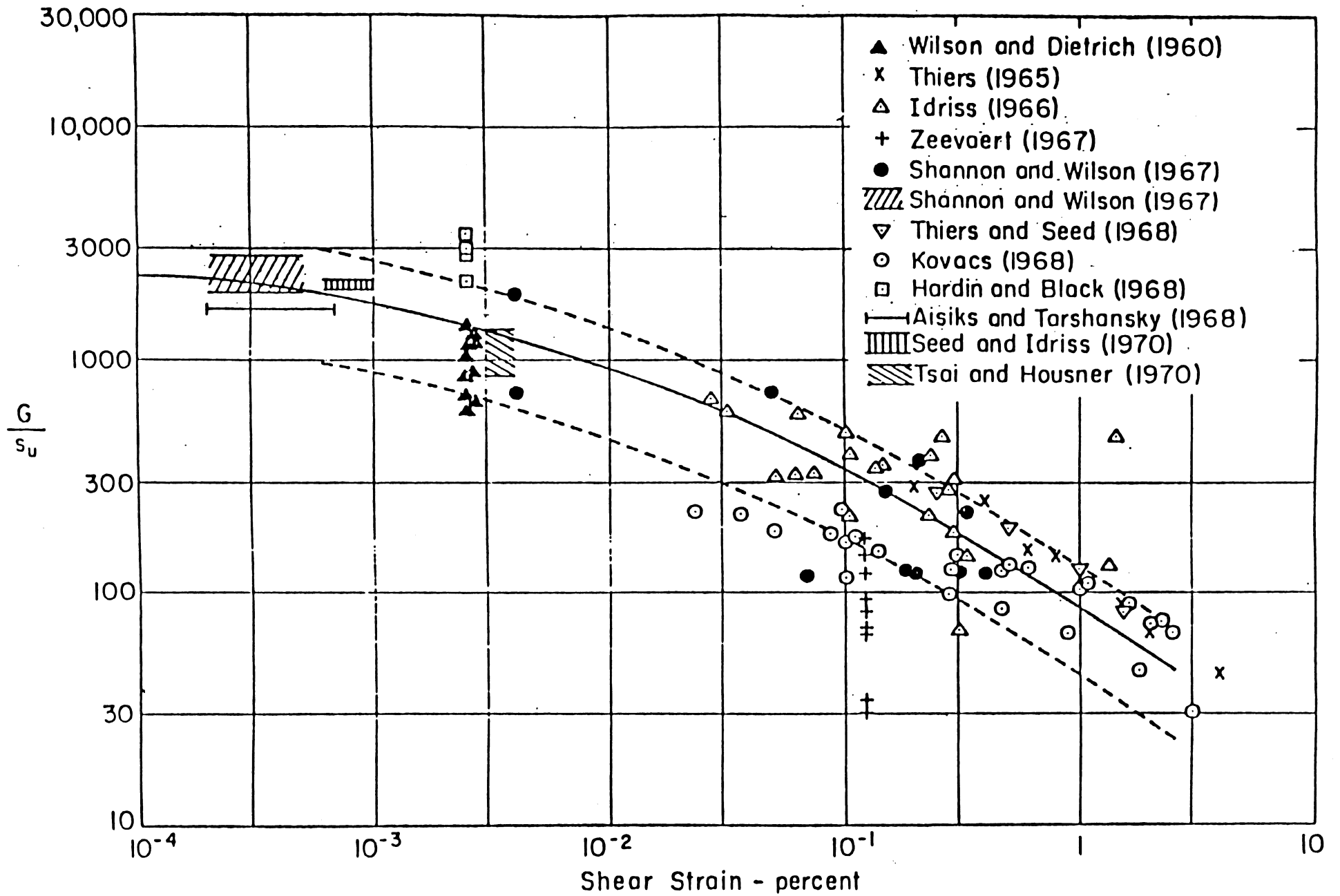


Fig. 3. IN-SITU SHEAR MODULI FOR SATURATED CLAYS  
(FROM SEED AND IDRIS, 1970)

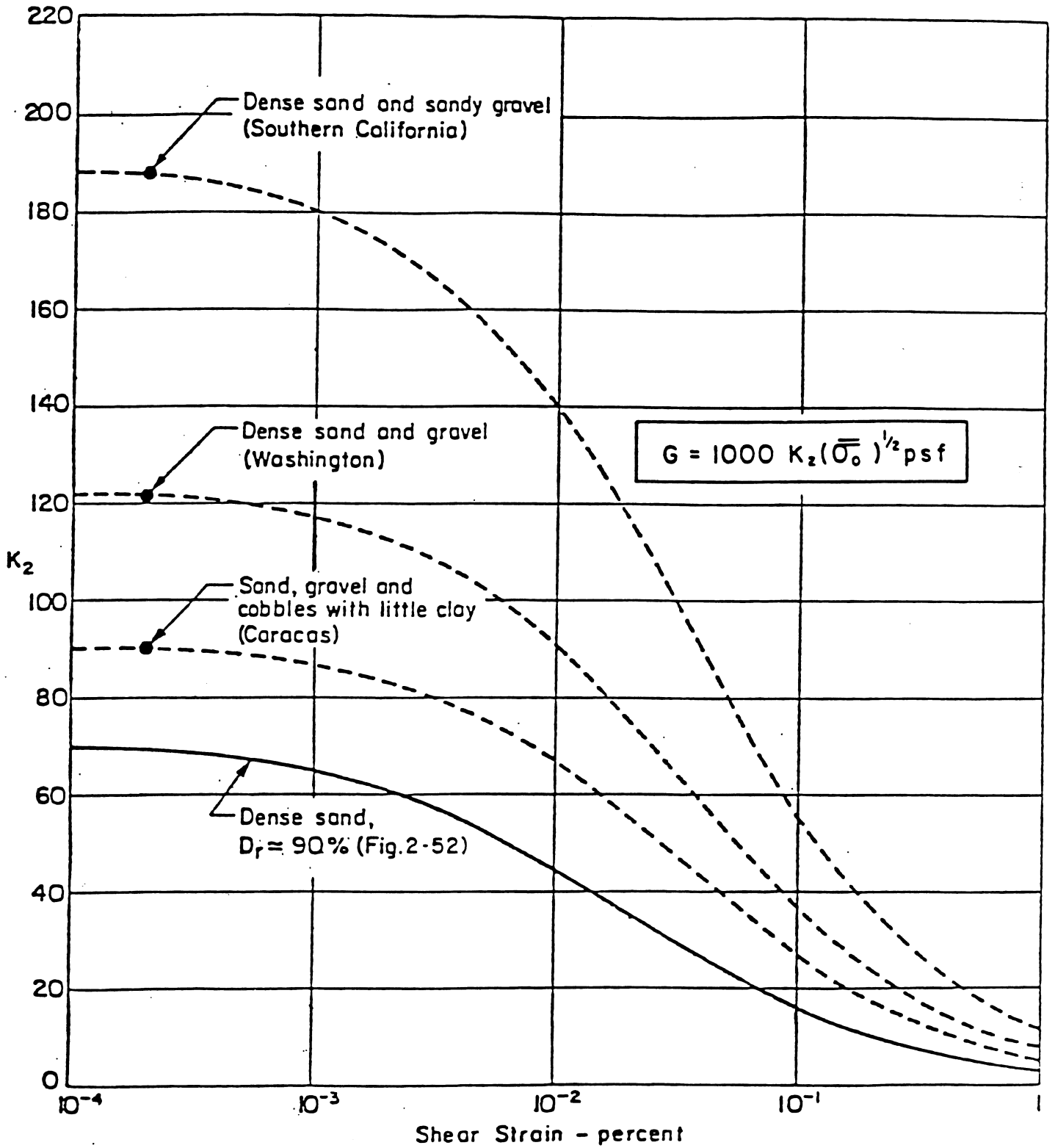


Fig. 4. MODULI DETERMINATIONS FOR GRAVELLY SOILS  
(AFTER SEED AND IDRIS, 1970)

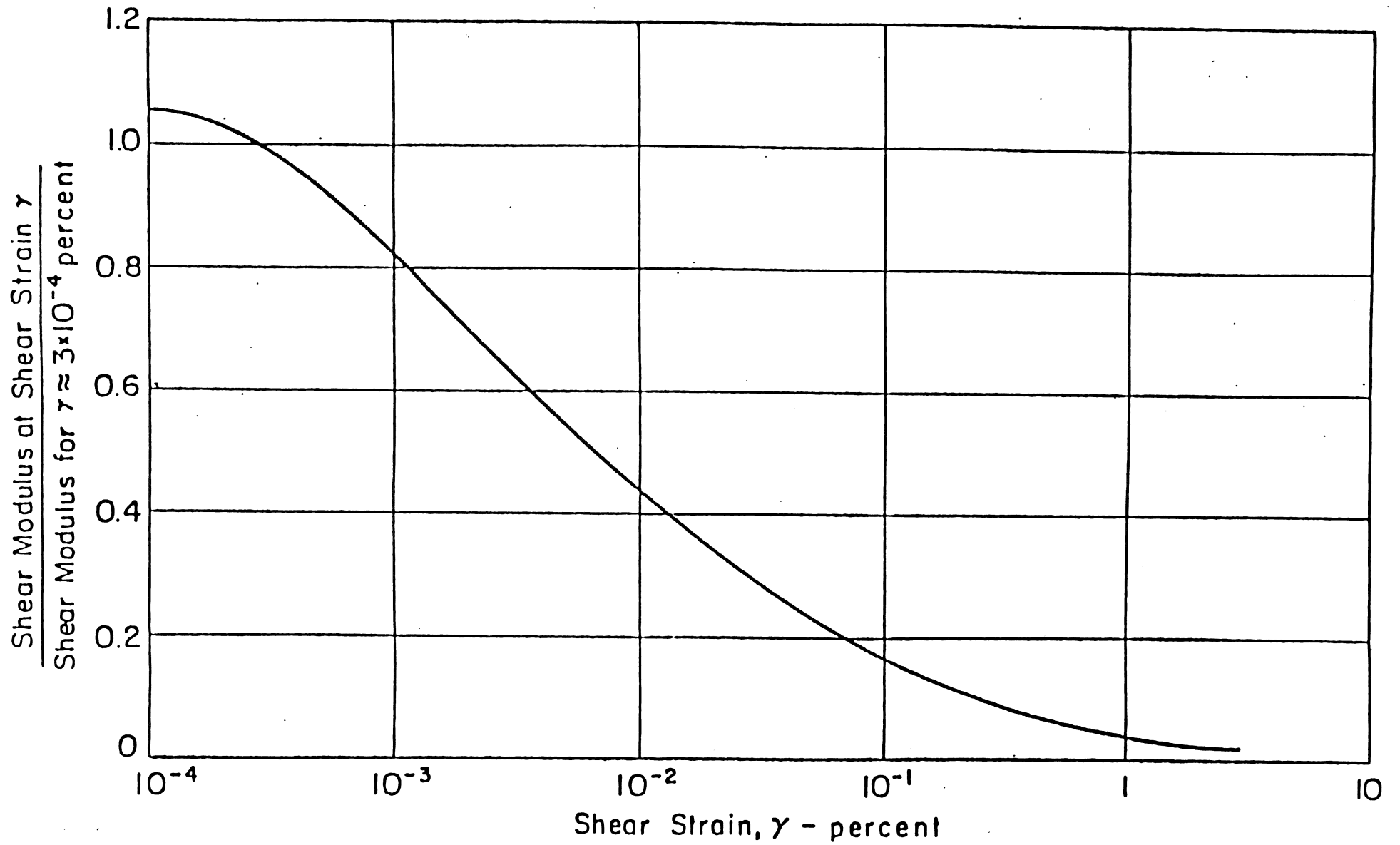


Fig. 5. TYPICAL REDUCTION OF SHEAR MODULUS WITH SHEAR STRAIN FOR SATURATED CLAYS  
(AFTER SEED AND IDRISSE, 1970)

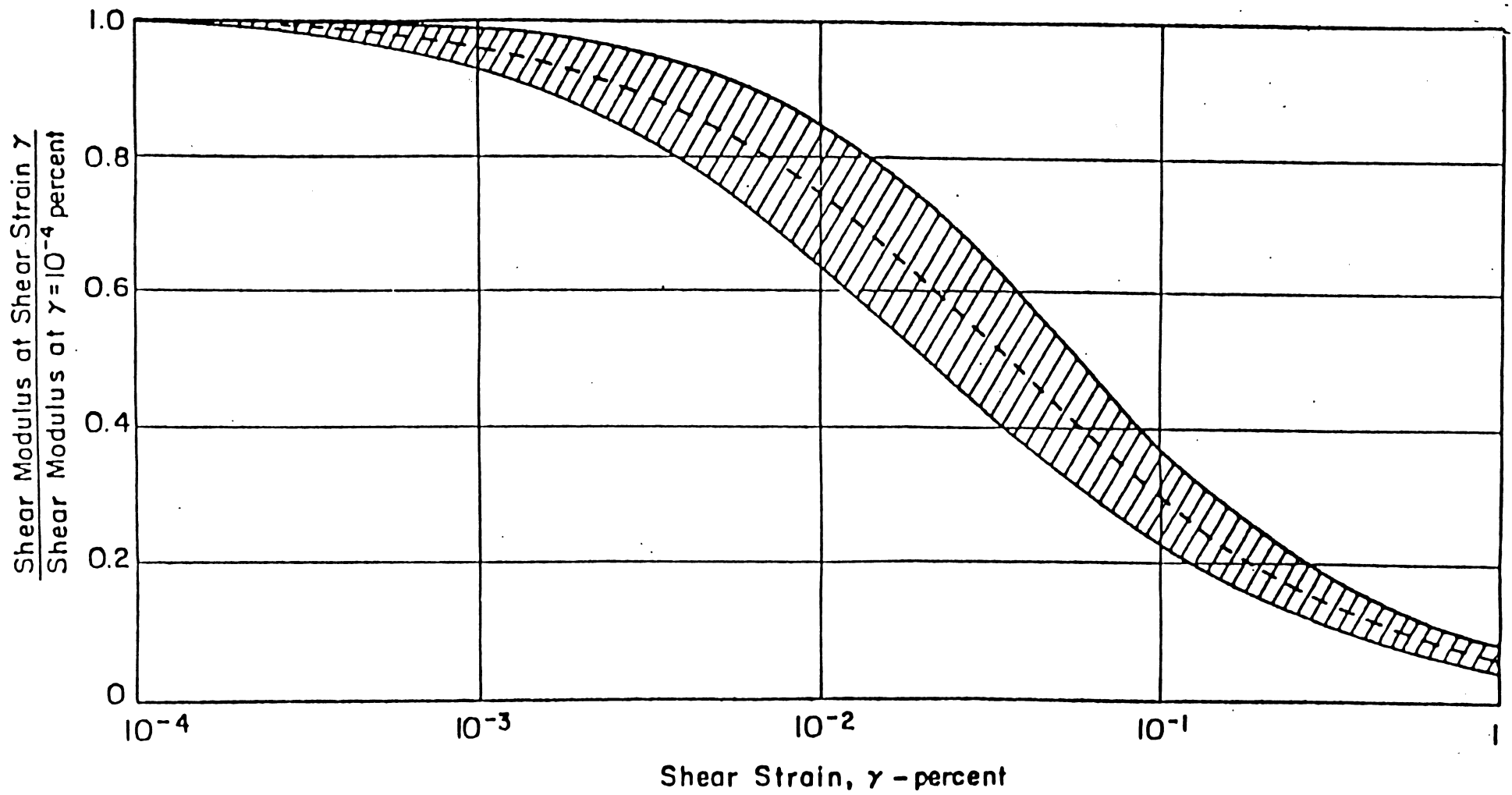


Fig. 6. VARIATION OF SHEAR MODULUS WITH SHEAR STRAIN FOR SANDS  
(AFTER SEED AND IDRIS, 1970)

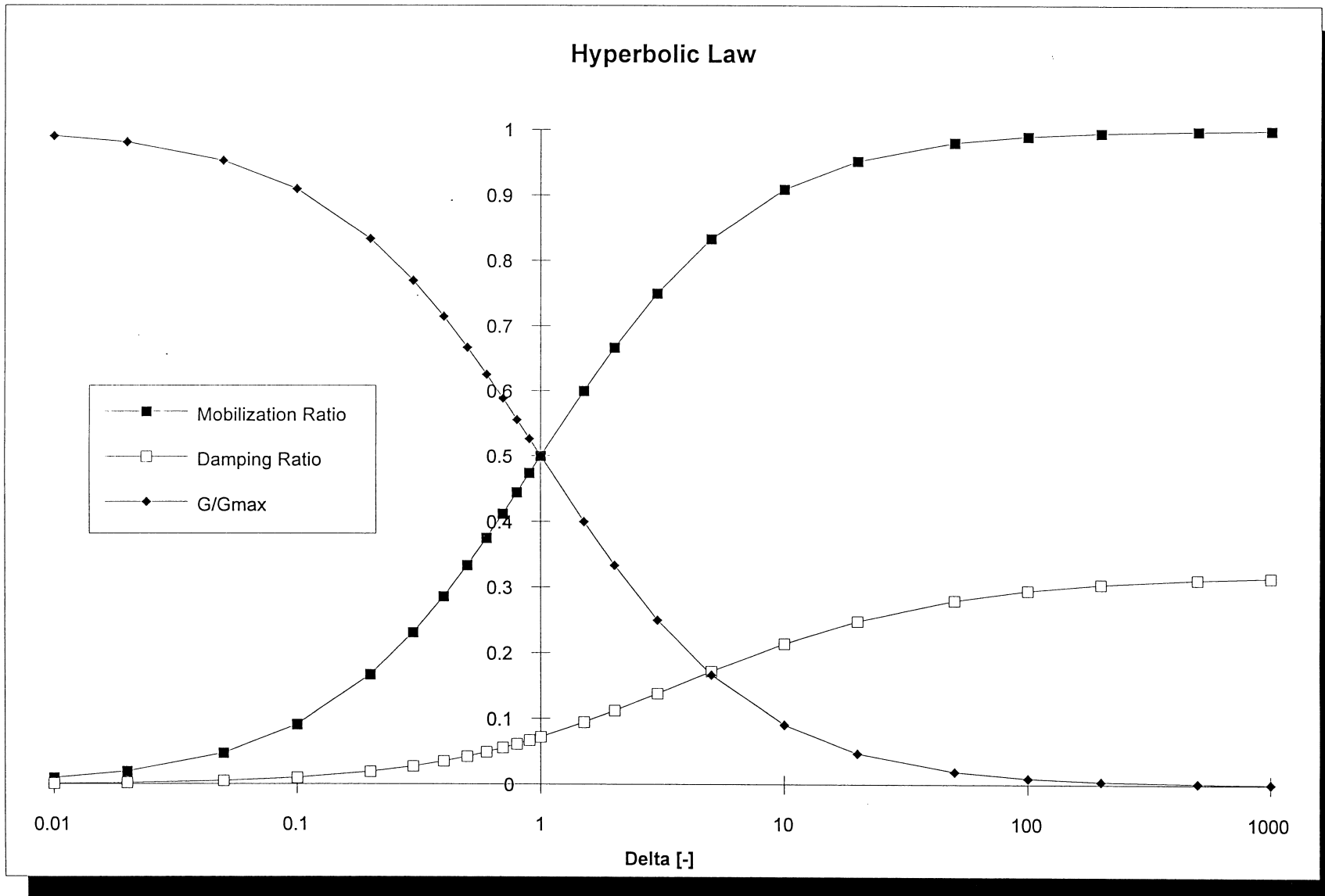


Fig. 7. Hyperbolic Law (Chart 5)

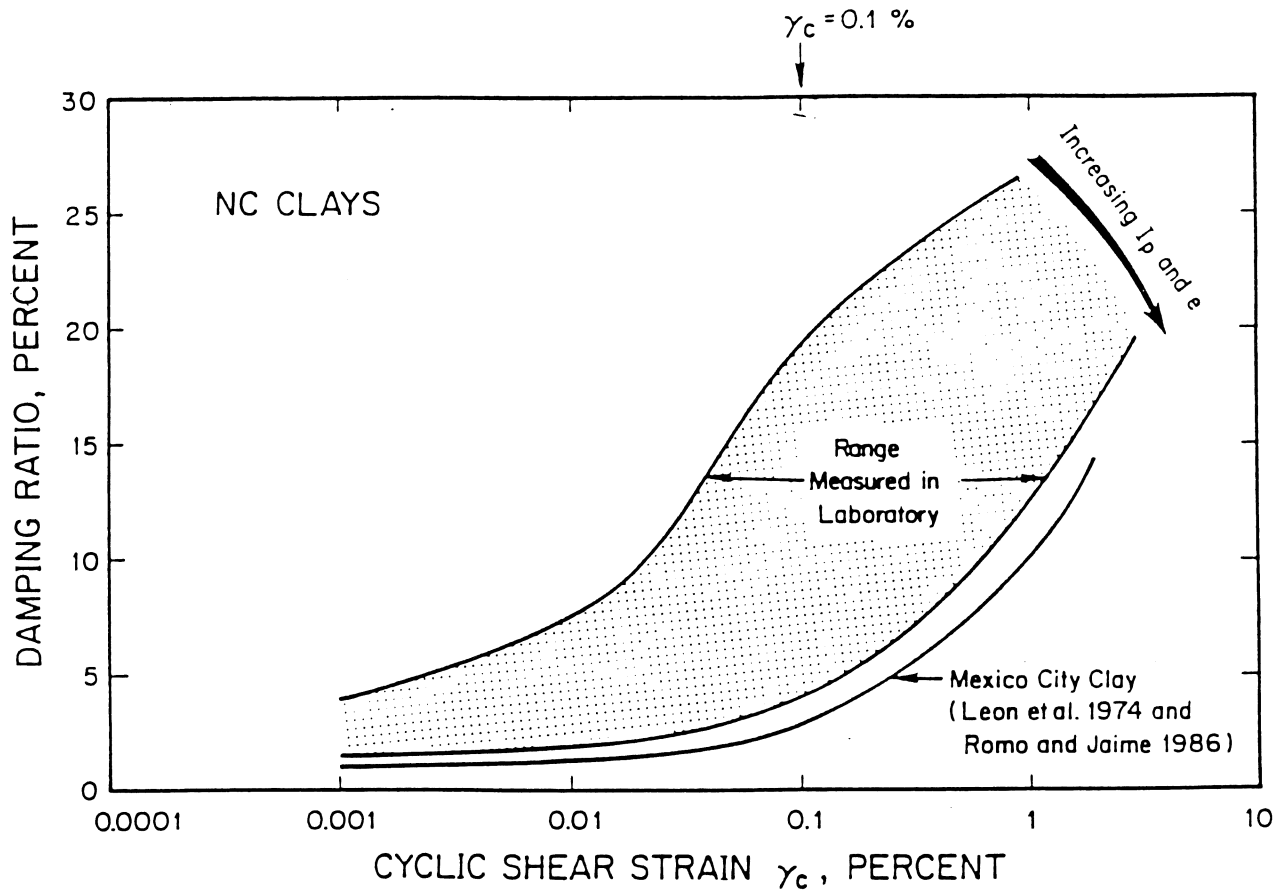


Fig. 8. Damping Ratio Range and Trends Measured in Clays in the Laboratory. (Dobry and Vucetic, 1987)

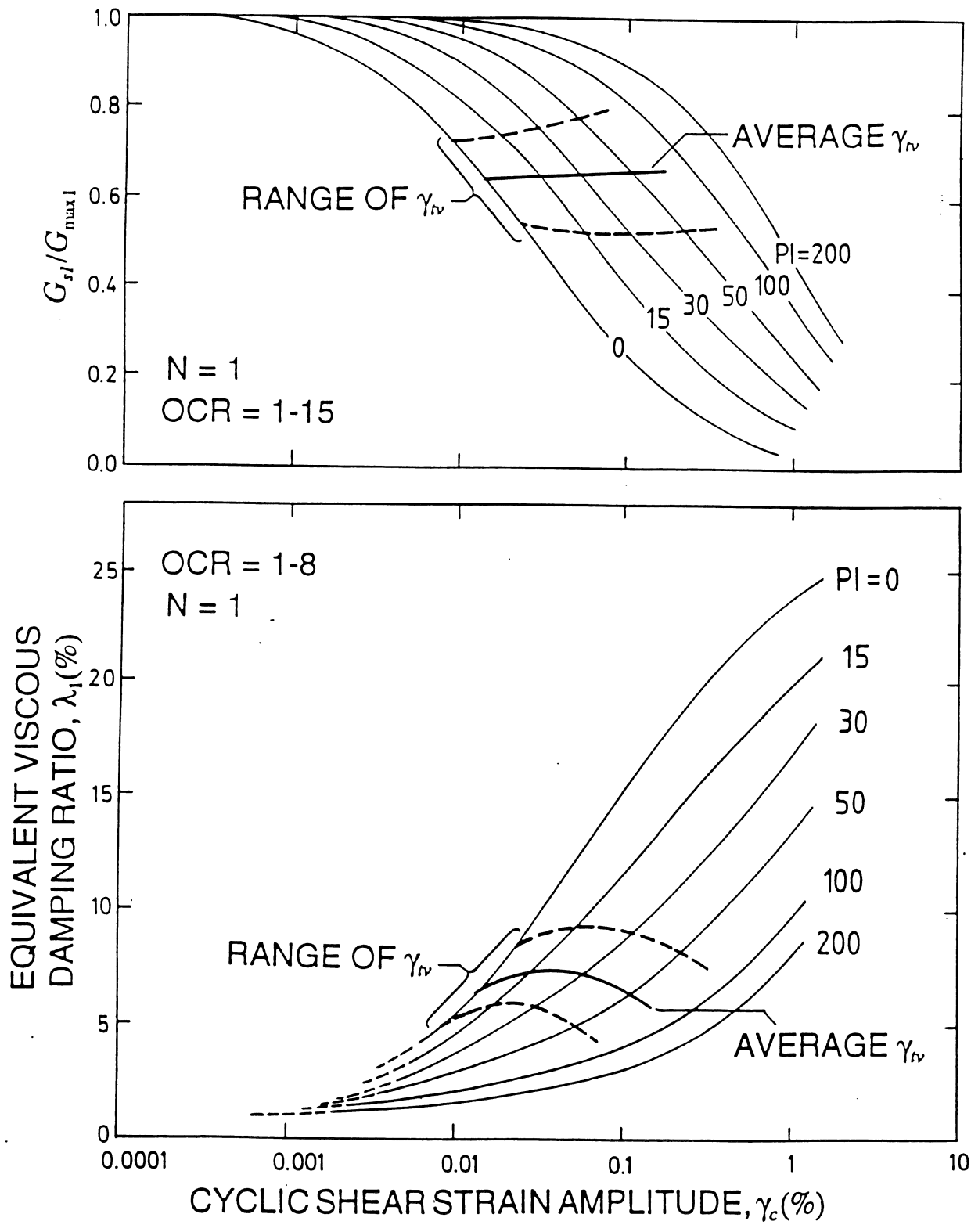


Figure 9. Relation between  $\gamma_{nv}$  and Modulus Reduction and Damping Curves for Fully Saturated Soils Cyclically Sheared in Undrained Conditions (modified from Vucetic and Dobry, 1991)

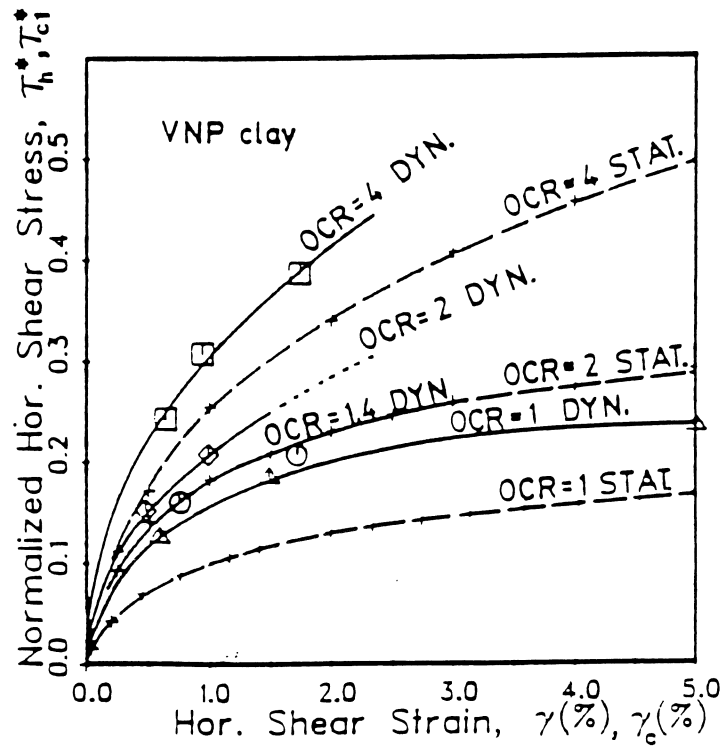


Fig. 10. Comparison of Static and Dynamic tests Results (Dobry and Vucetic, 1987)

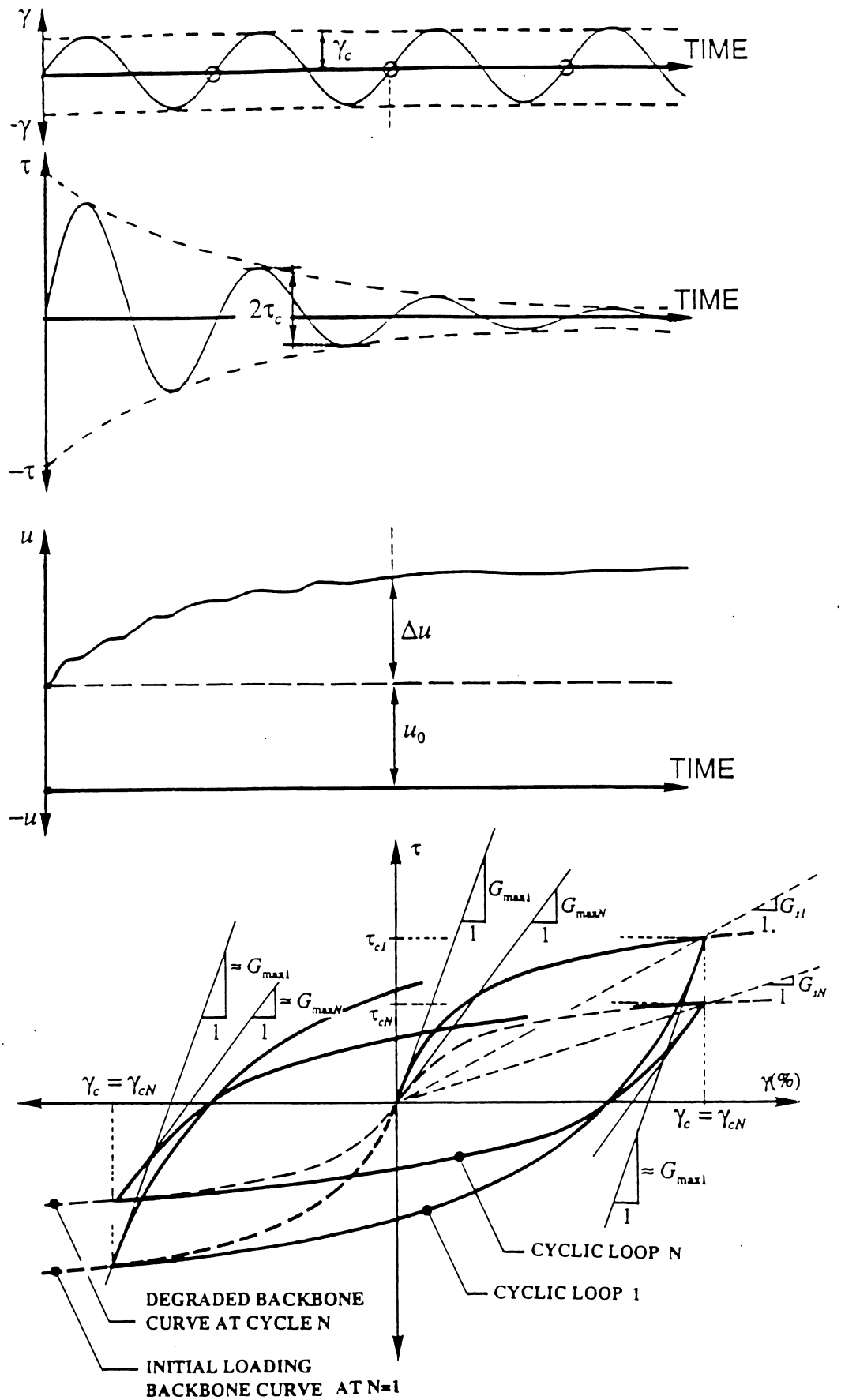


Figure 11. Sketch of the Results and the Definition of Parameters of a Cyclic Strain-Controlled Simple Shear Test on NC Clay

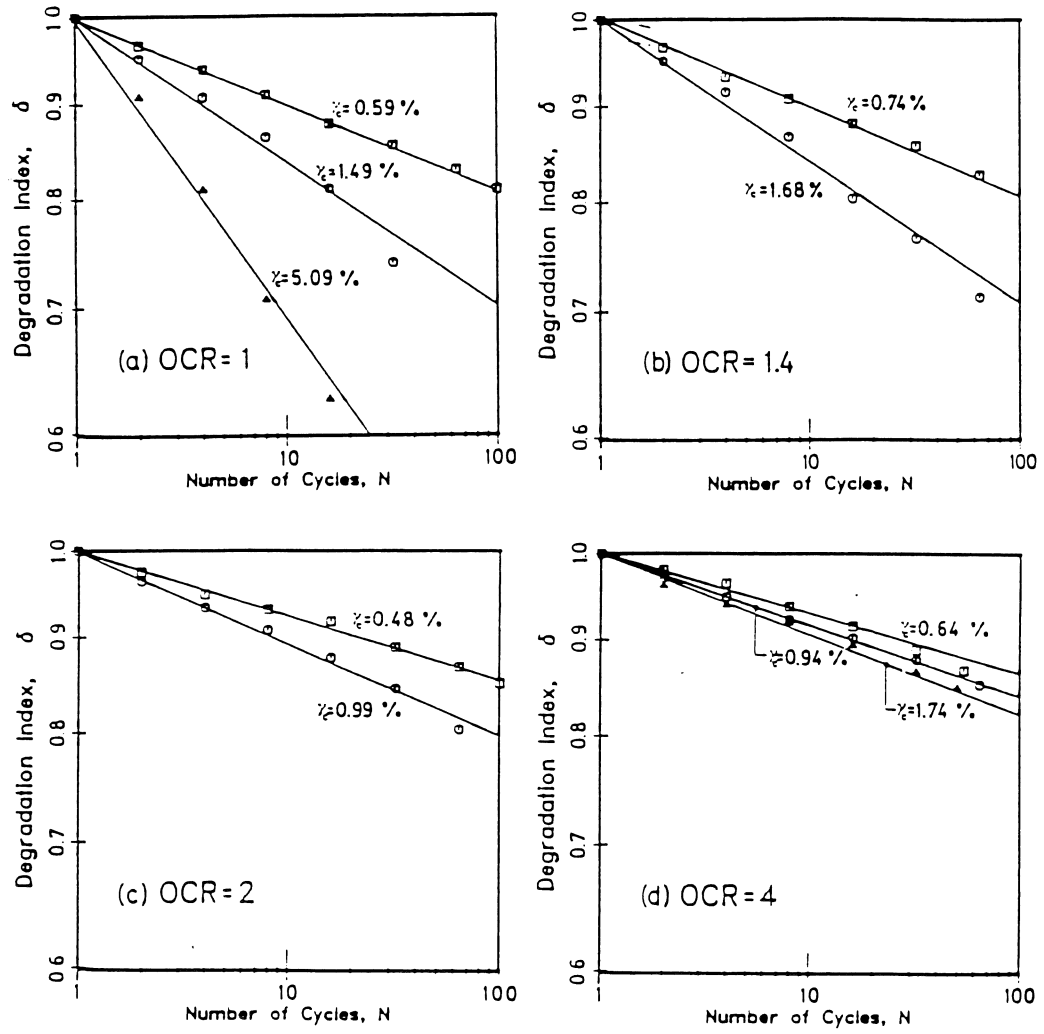
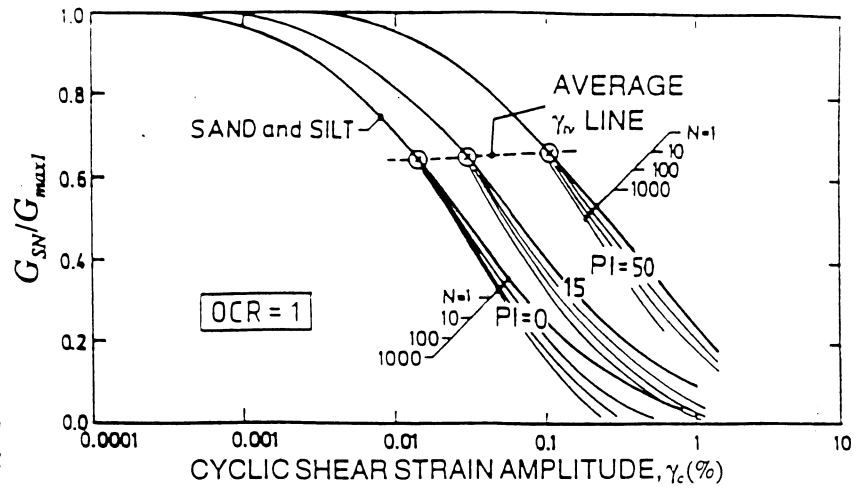
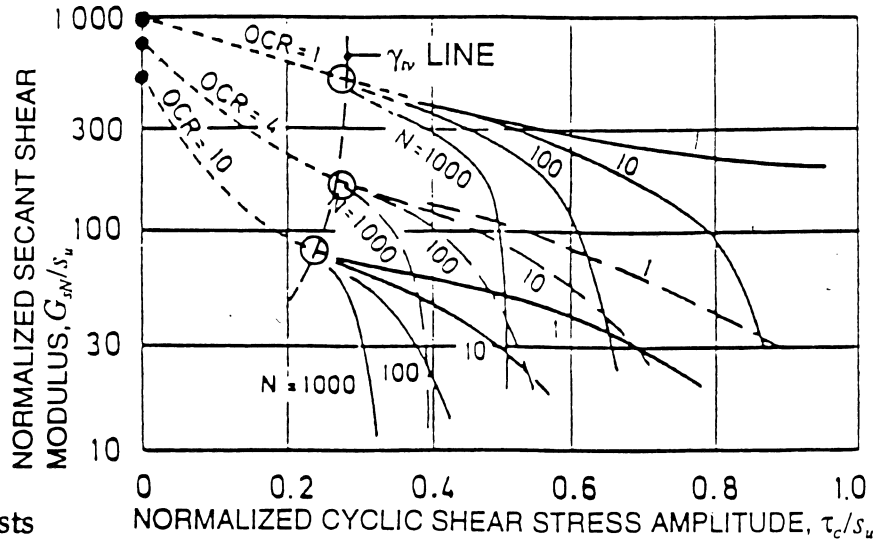


Fig. 12. Degradation Index Versus number of cycles (Dobry and Vucetic, 1987)

a) Results of Cyclic Strain-Controlled Tests on Different Soils (modified from Vucetic and Dobry, 1991)



b) Results of Cyclic Stress-Controlled Tests on Clay (modified from Andersen, 1983)



c) Effect of the Plasticity Index on the Degradation Parameter,  $r$ , for Normally Consolidated Clays

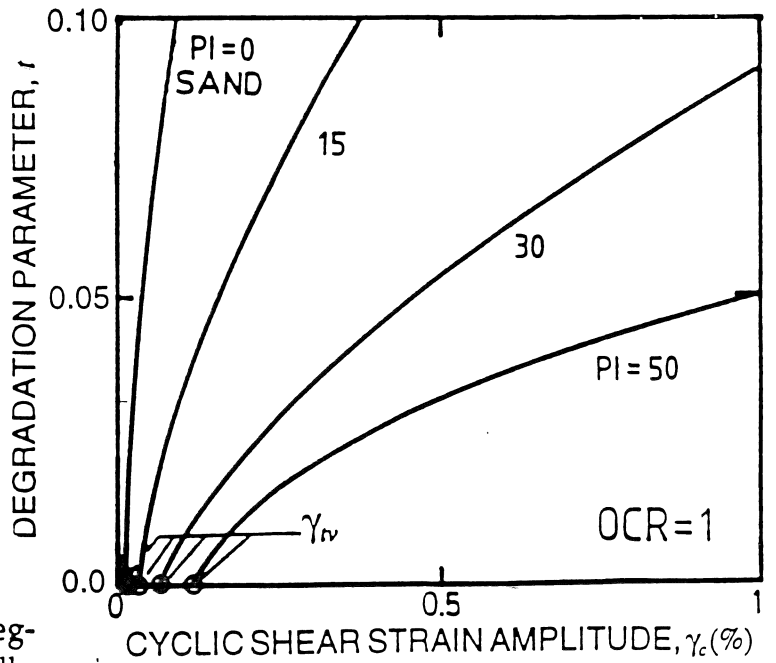


Figure 13. Relations between  $\gamma_{rv}$  and Cyclic Degradation (Vucetic, 1993)

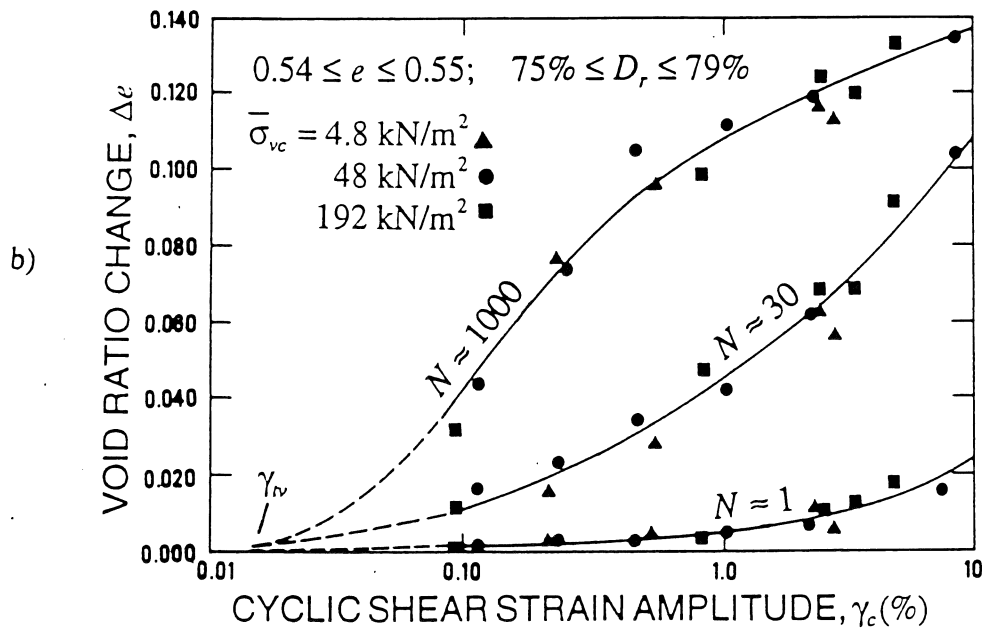
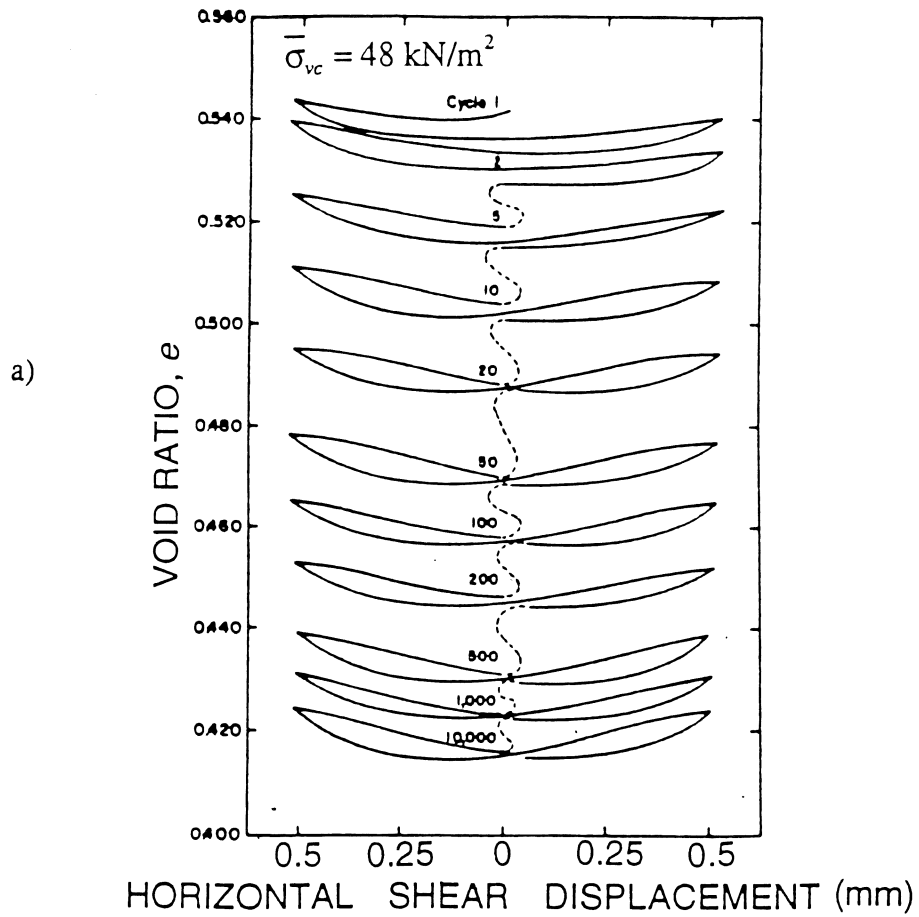


Figure 14. Volume Change of Fully Saturated Sand (Expressed in Terms of the Void Ratio Variation) in Cyclic Strain-Controlled Drained Simple Shear Test (Youd, 1972)

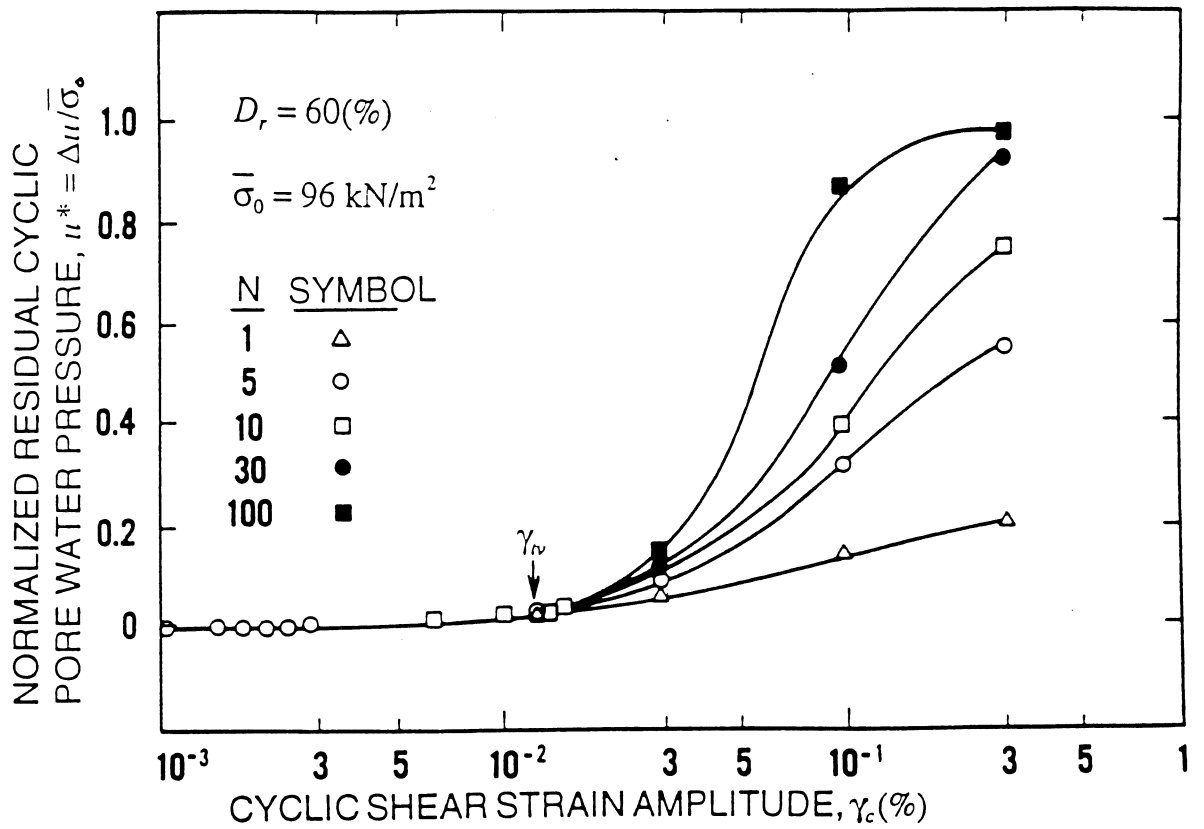


Figure 15a. Buildup of Residual Pore Water Pressure in Sand in Cyclic Triaxial Strain-Controlled Test (Dobry et al., 1982)

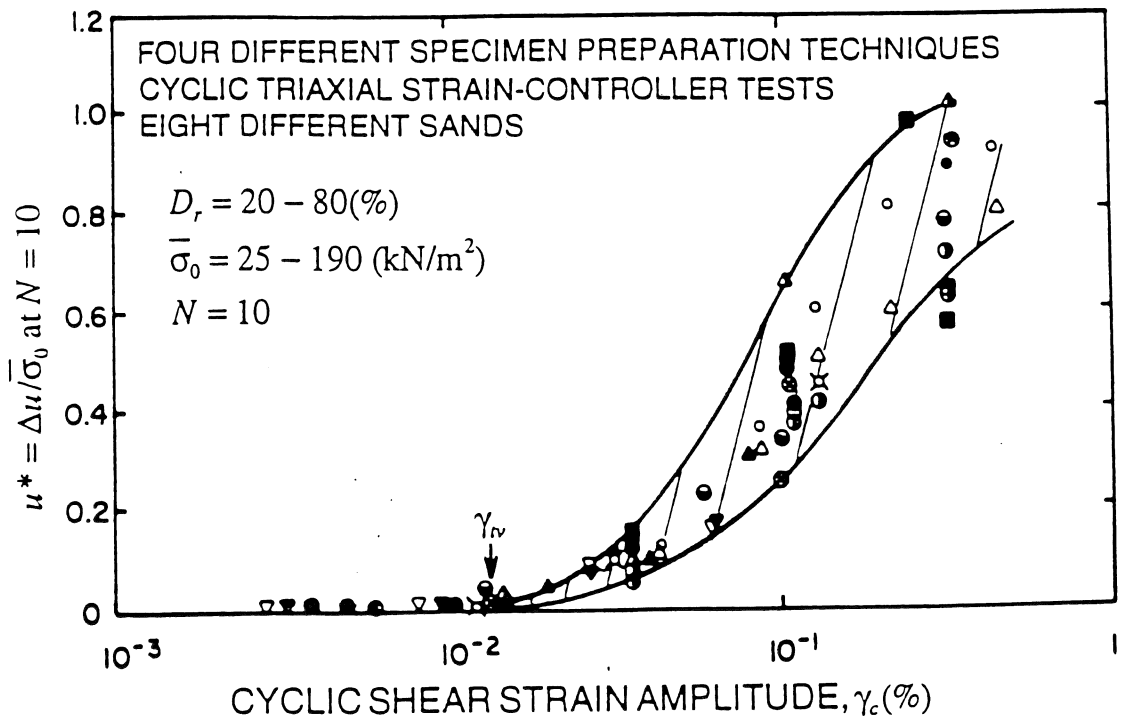


Figure 15b. Buildup of Residual Pore Water Pressure in Different Sands in Cyclic Triaxial Strain-Controlled Test (Presented by Dobry in NRC, 1985)

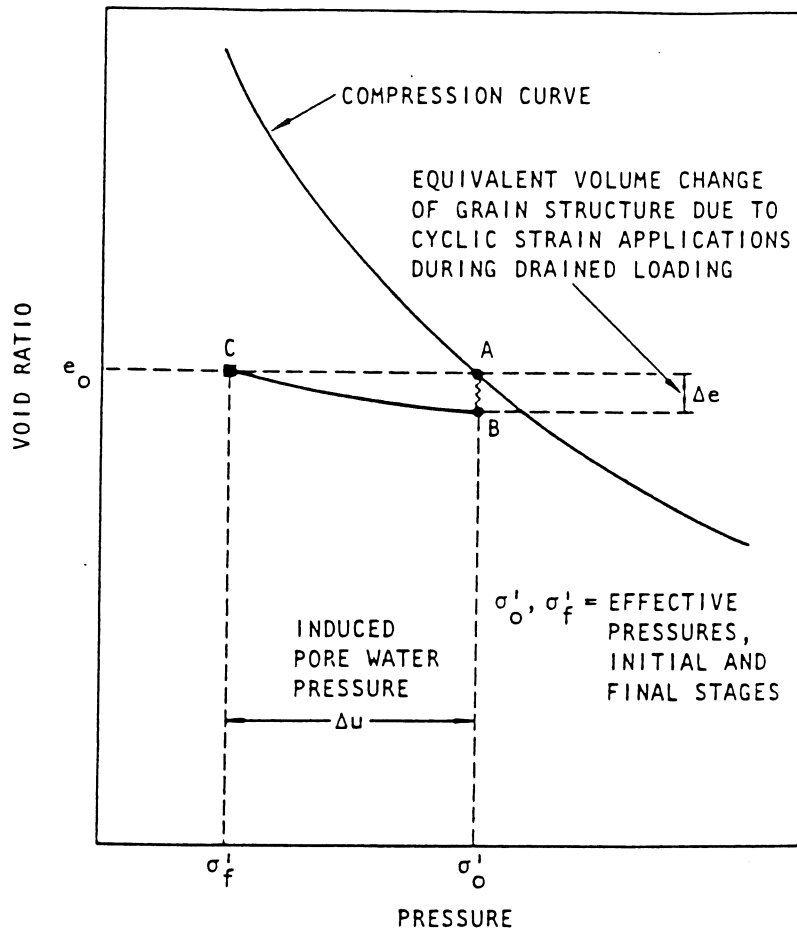


FIGURE 16. Schematic illustration of mechanism of pore pressure generation during cyclic loading. Source: Seed and Idriss (1982).

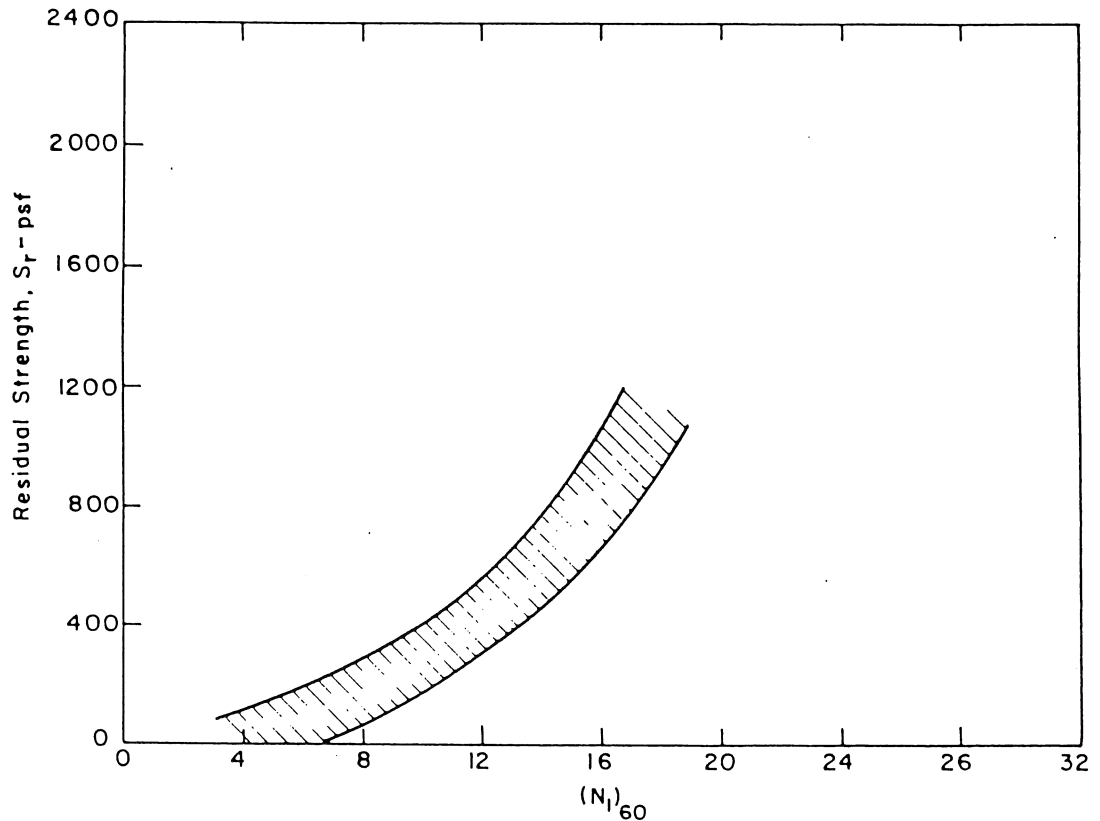
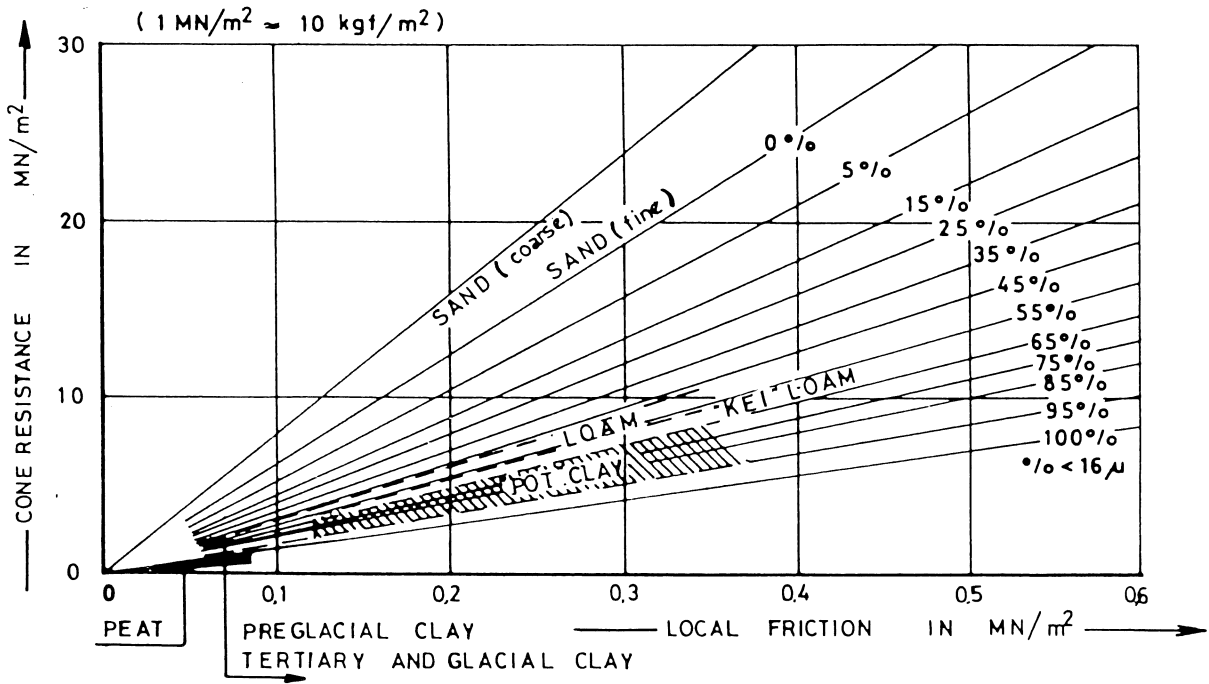
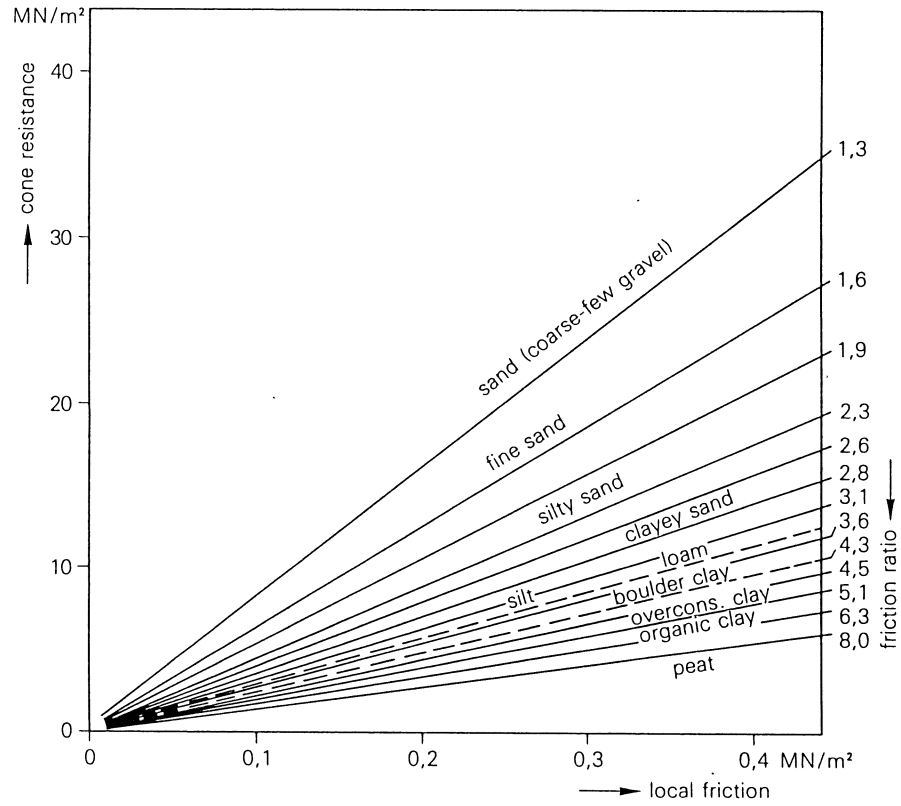


FIGURE 17. Tentative relationship between residual strength and SPT  $N$ -value. Source: Seed (1984).



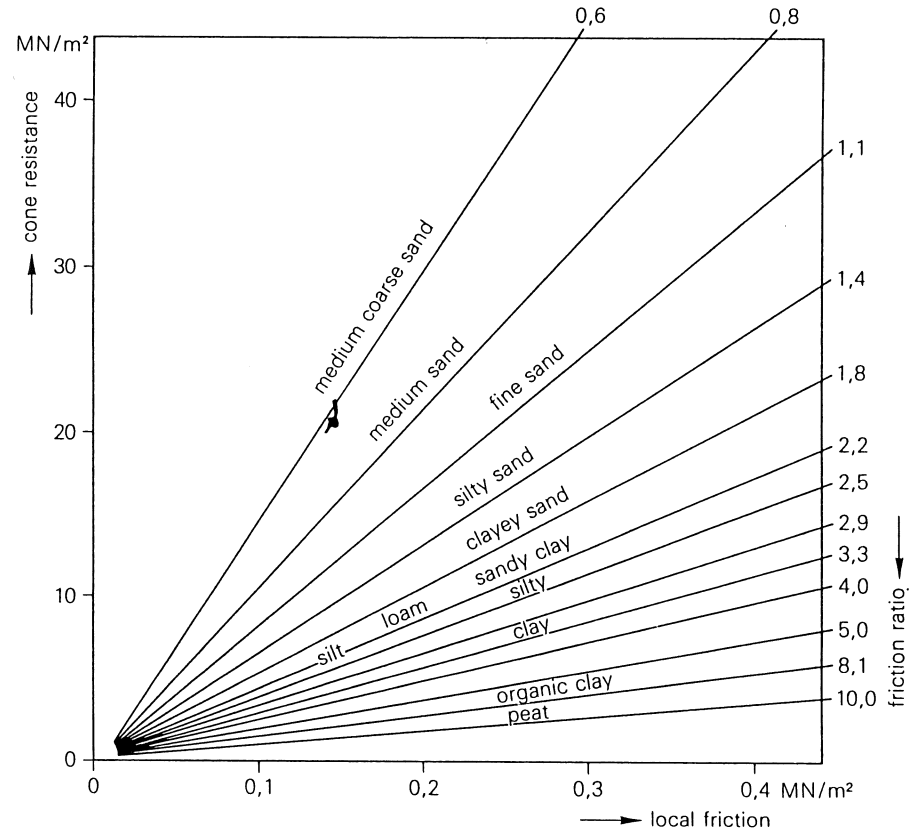
Information on soil strata provided by the ratio of cone resistance and local friction.

Fig. 18. Friction Ratio Correlations with fines content



Verband tussen grootte van het wrijvingsgetal en de grondsoort voor de mechanische kleefmantelconus

Relation between the friction ratio and the type of soil for the mechanical adhesion jacket cone



Verband tussen grootte van het wrijvingsgetal en de grondsoort voor de cilindrische elektrische kleefmantelconus

Relation between the friction ratio and the type of soil for the cylindrical electrical adhesion jacket cone

Fig. 18. Friction Ratio Correlations with fines content and PI (Cont.)

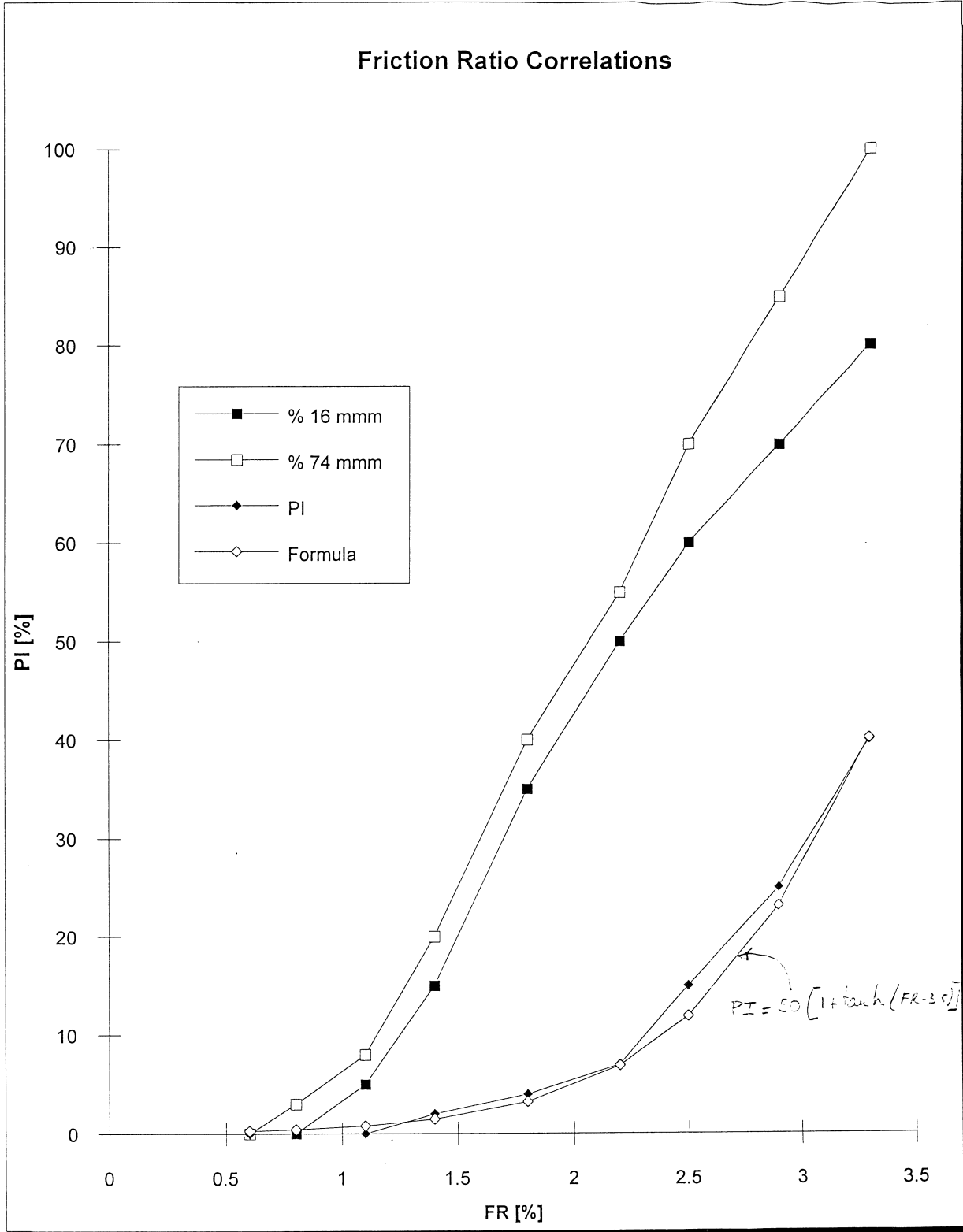


Fig. 18. Friction Ratio Correlations with fines content and PI (Chart 2)

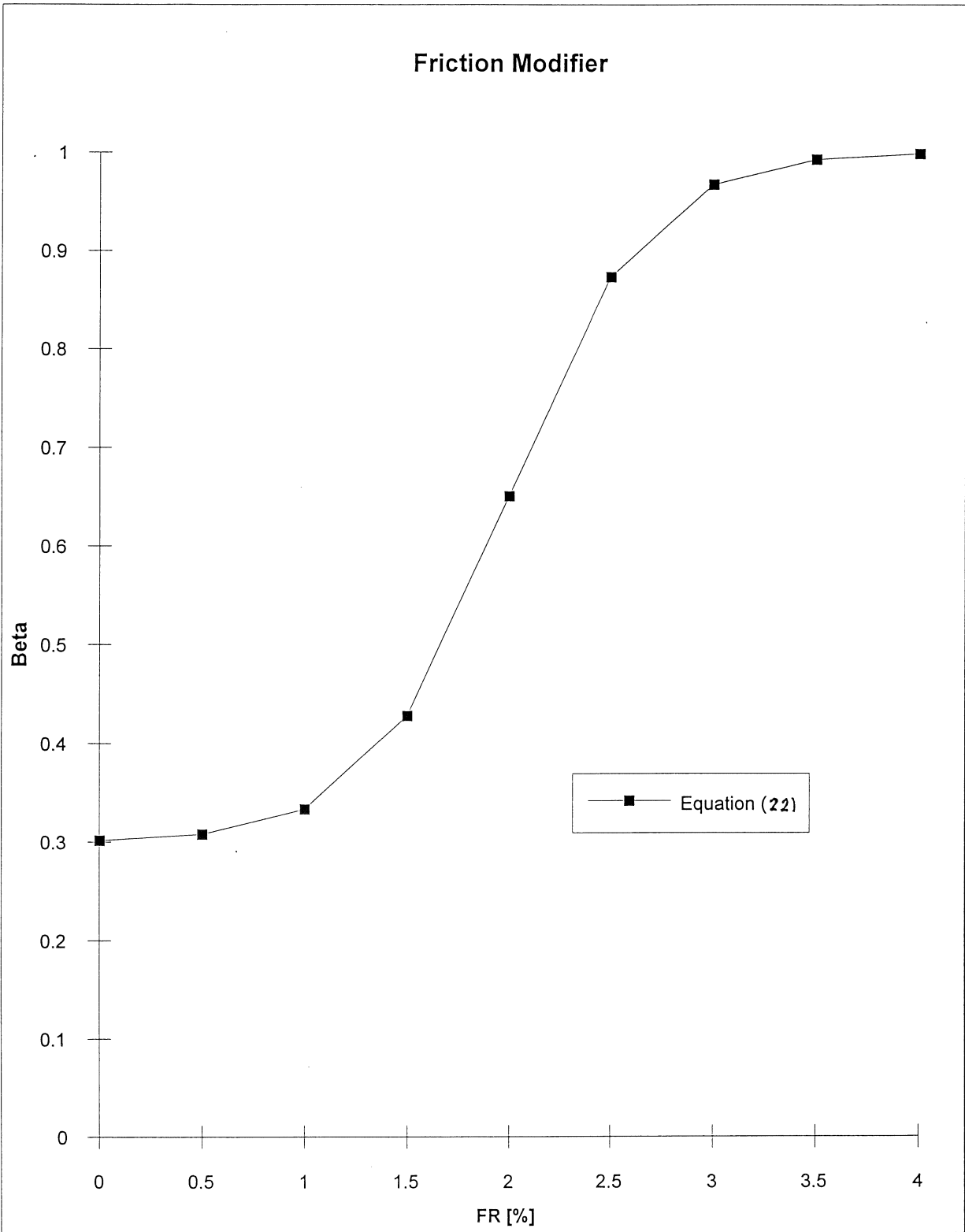


Fig. 19. Friction Modifier (Chart 3)

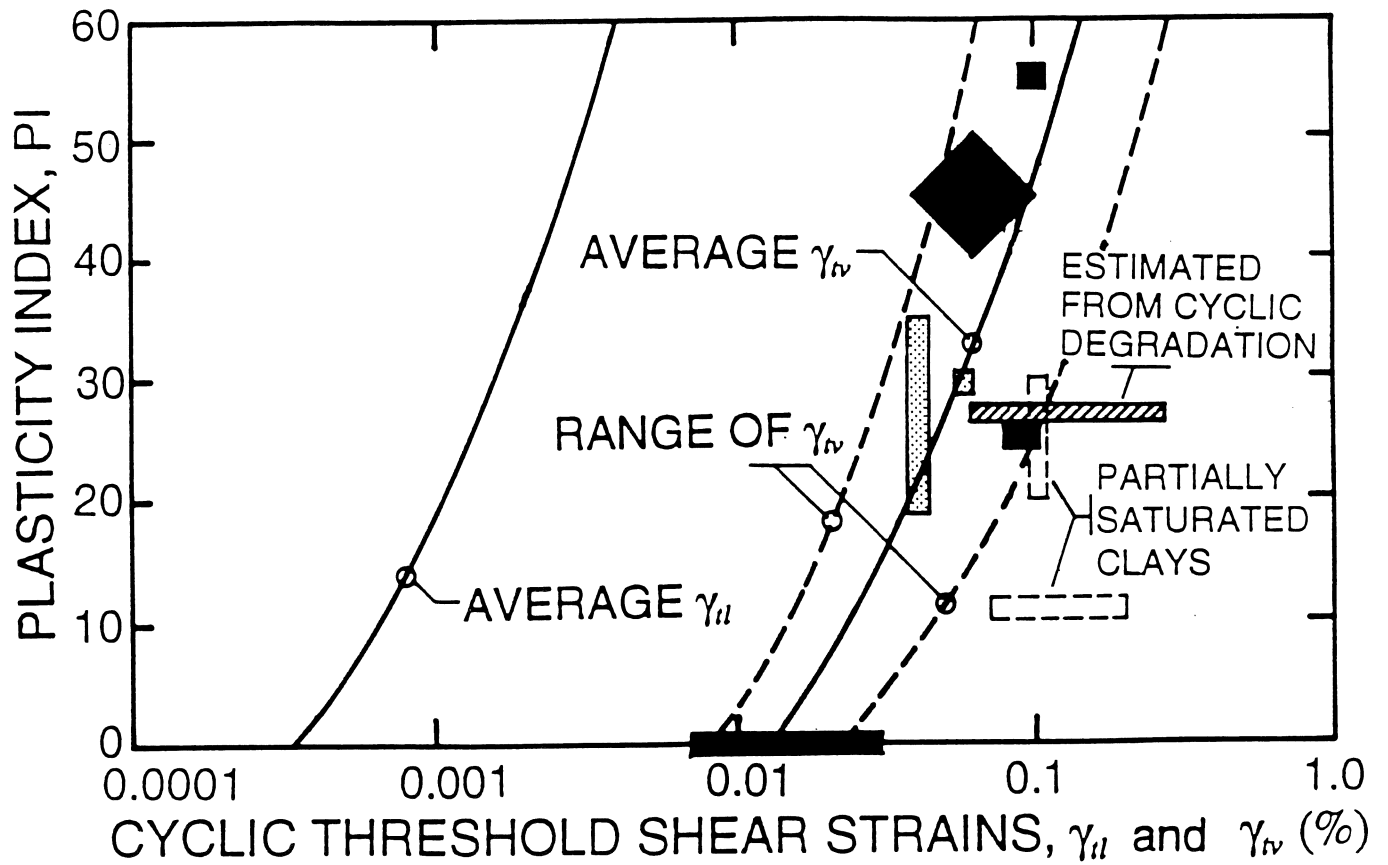


Fig. 20. Effect of the Plasticity Index on the Cyclic Threshold Shear Strains  $\gamma_{tl}$  and  $\gamma_{tv}$  (Vucetic, 1993)

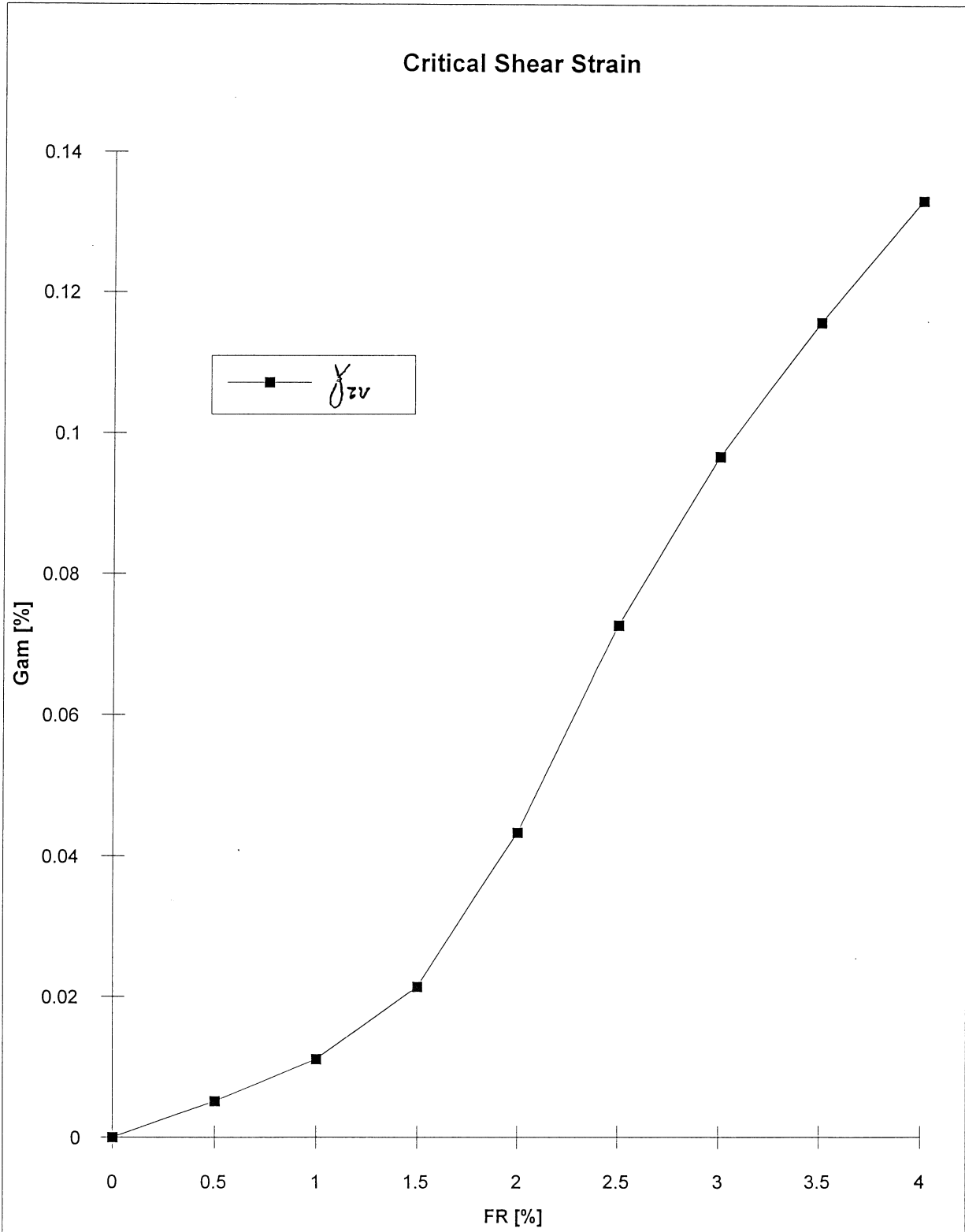


Fig. 21. Threshold Shear strain (Chart 4)

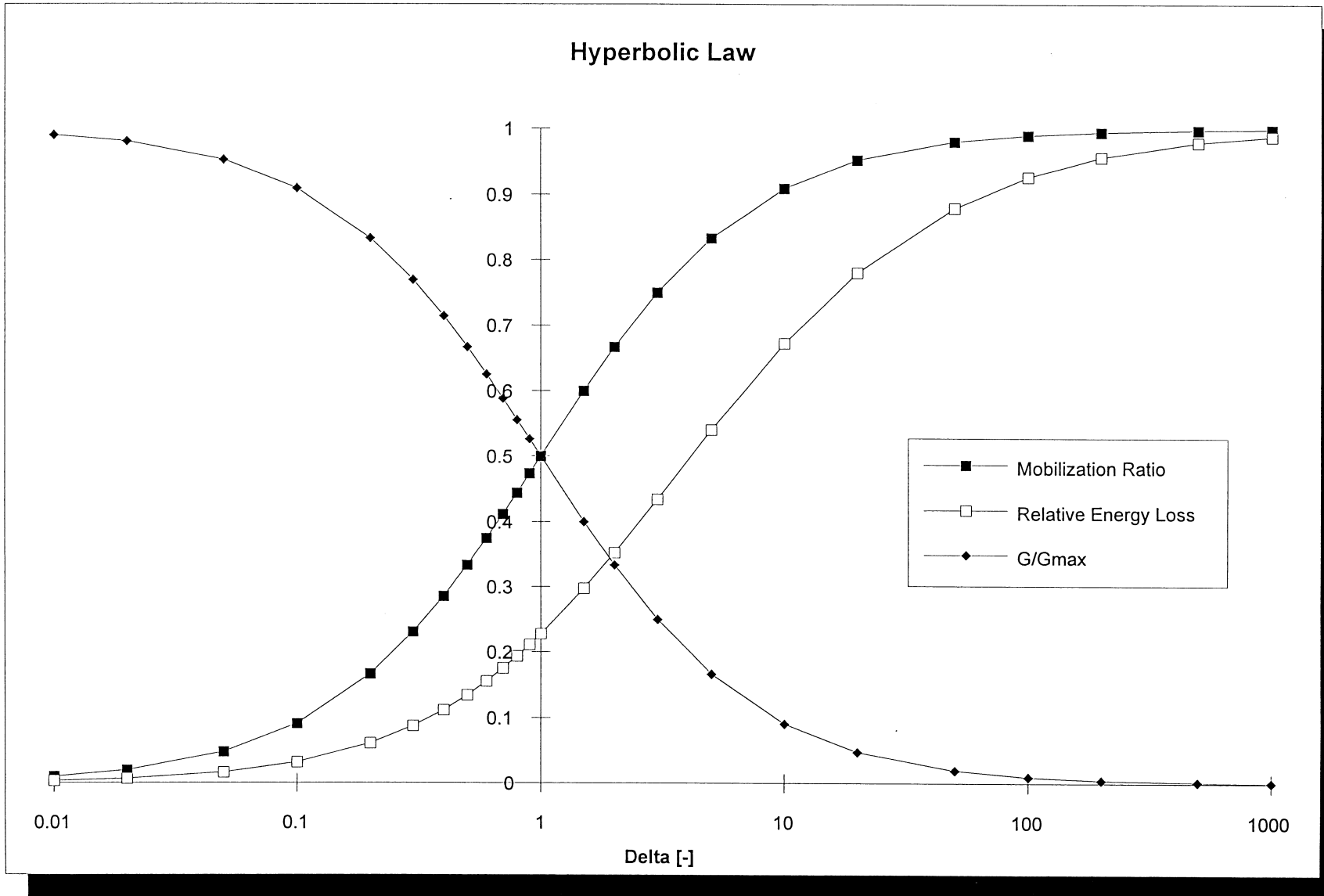


Fig. 22. Hyperbolic law to evaluate G/Gmax and Relative Energy Loss (Chart 5)

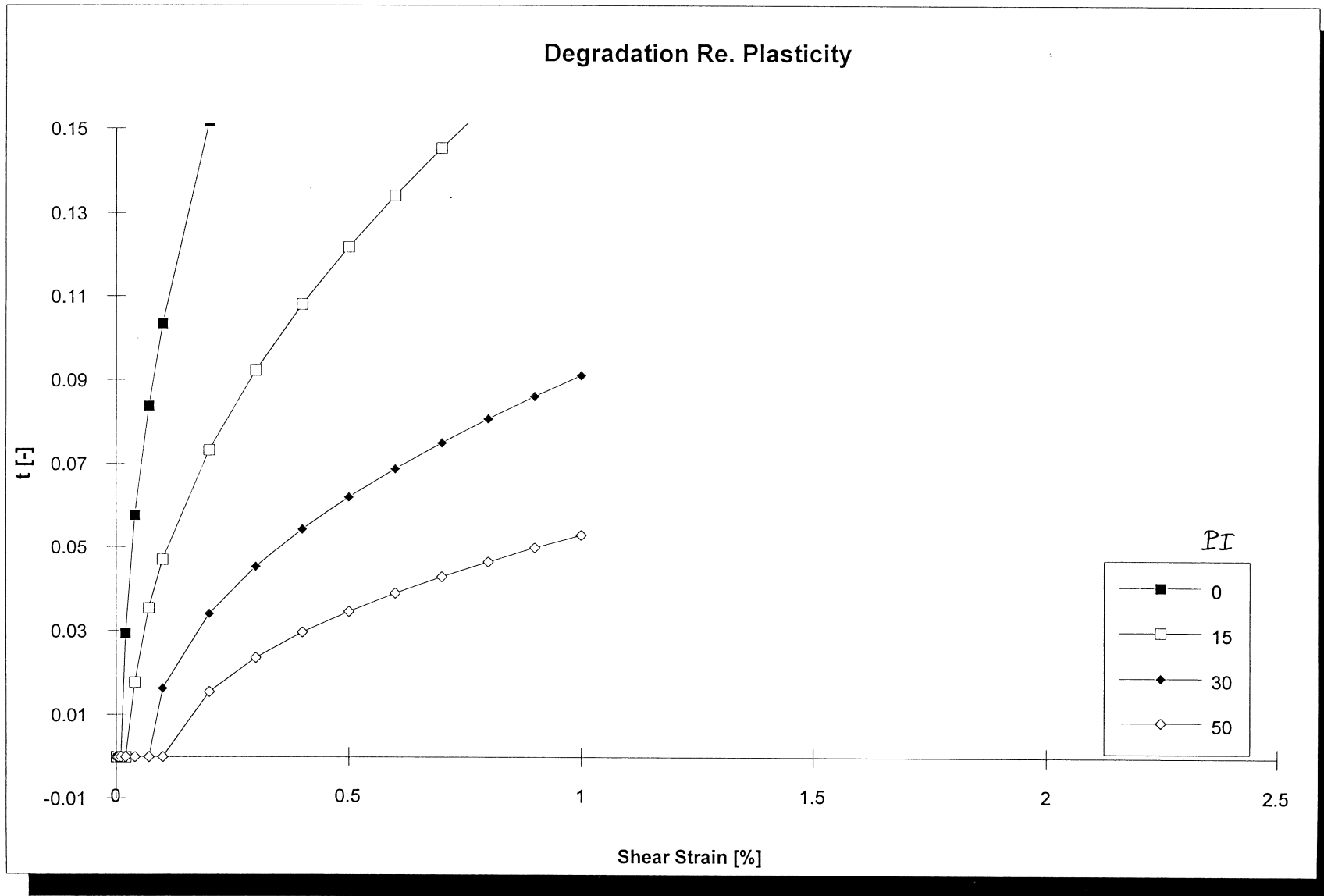


Fig. 23. Degradation Parameter Vs shear strain for different PI (Chart 6a)

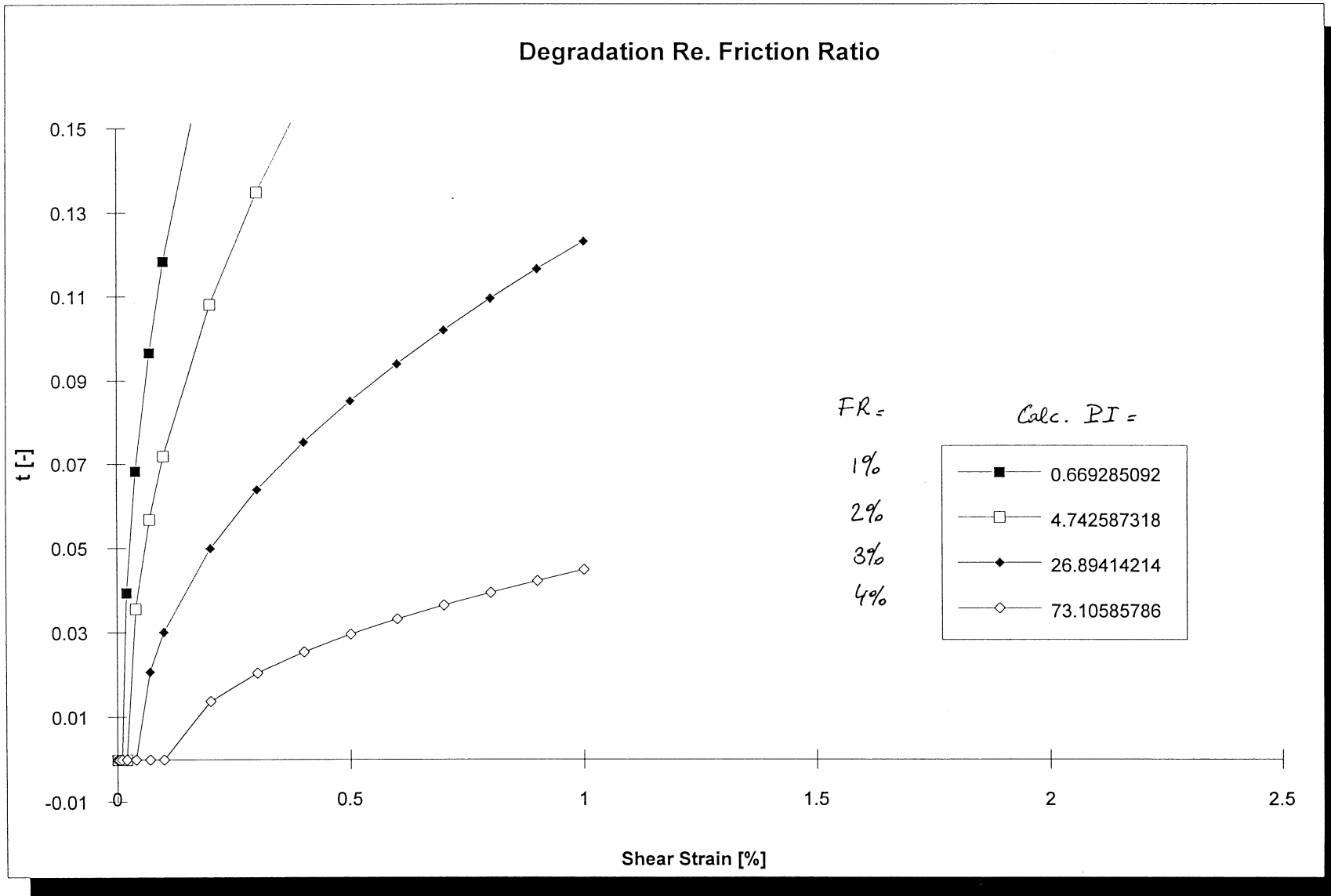


Fig. 24. Degradation Parameter Vs shear strain for different FR (Chart 6b)

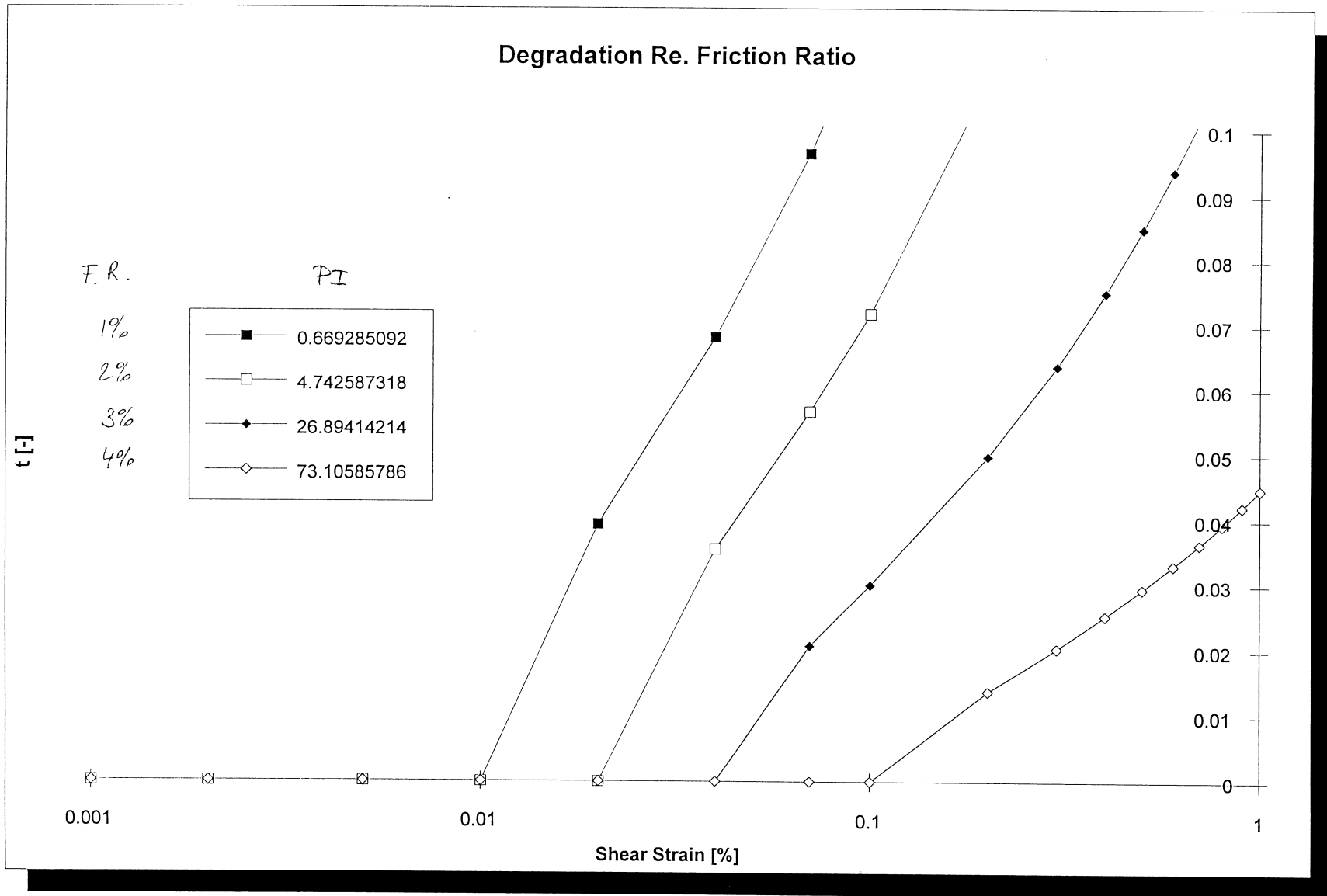


Fig. 25. Degradation Parameter Vs shear strain for different FR - Log scale(Chart 6c)

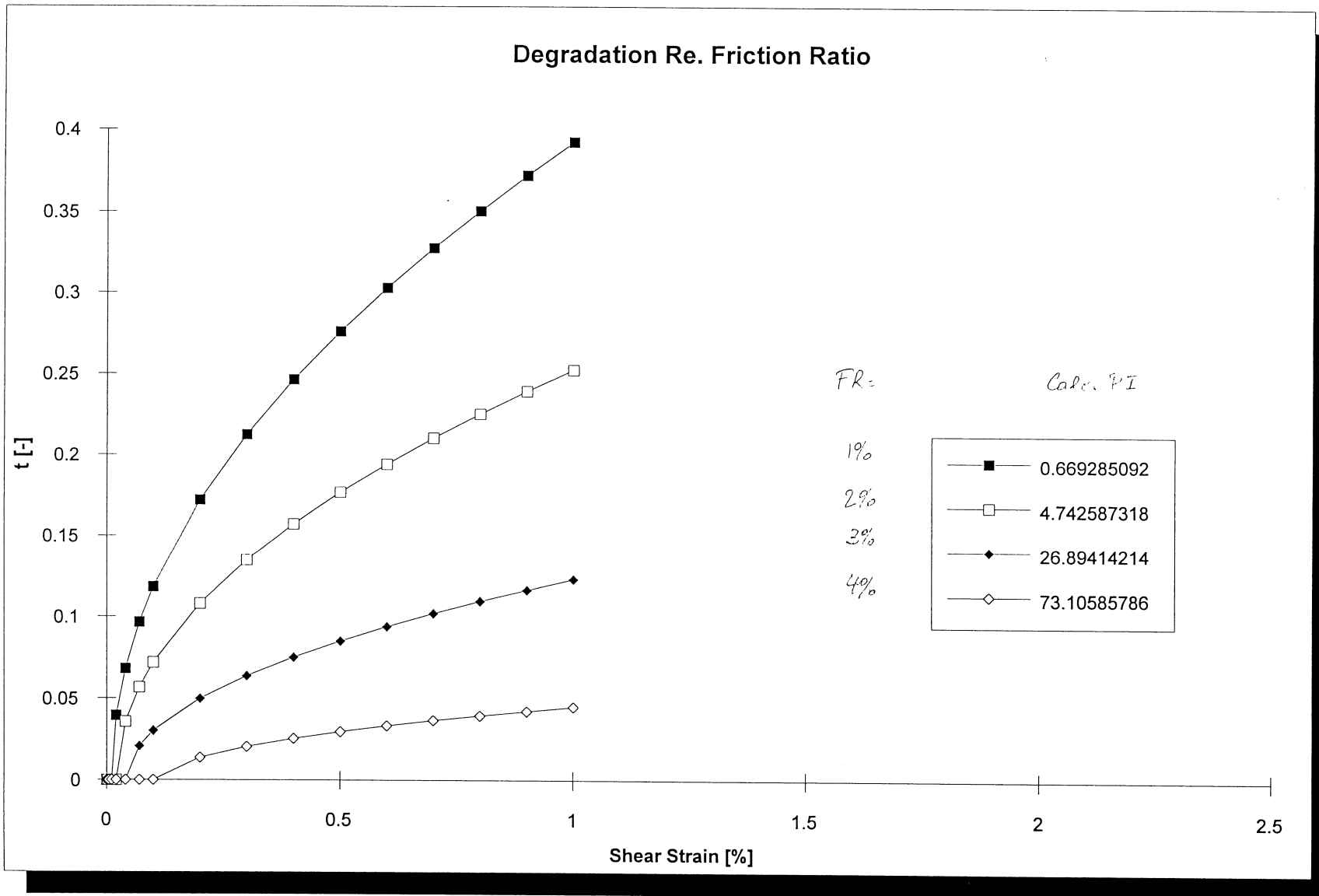


Fig. 27. Degradation Parameter - high values - Vs shear strain for different FR (Chart 6d)

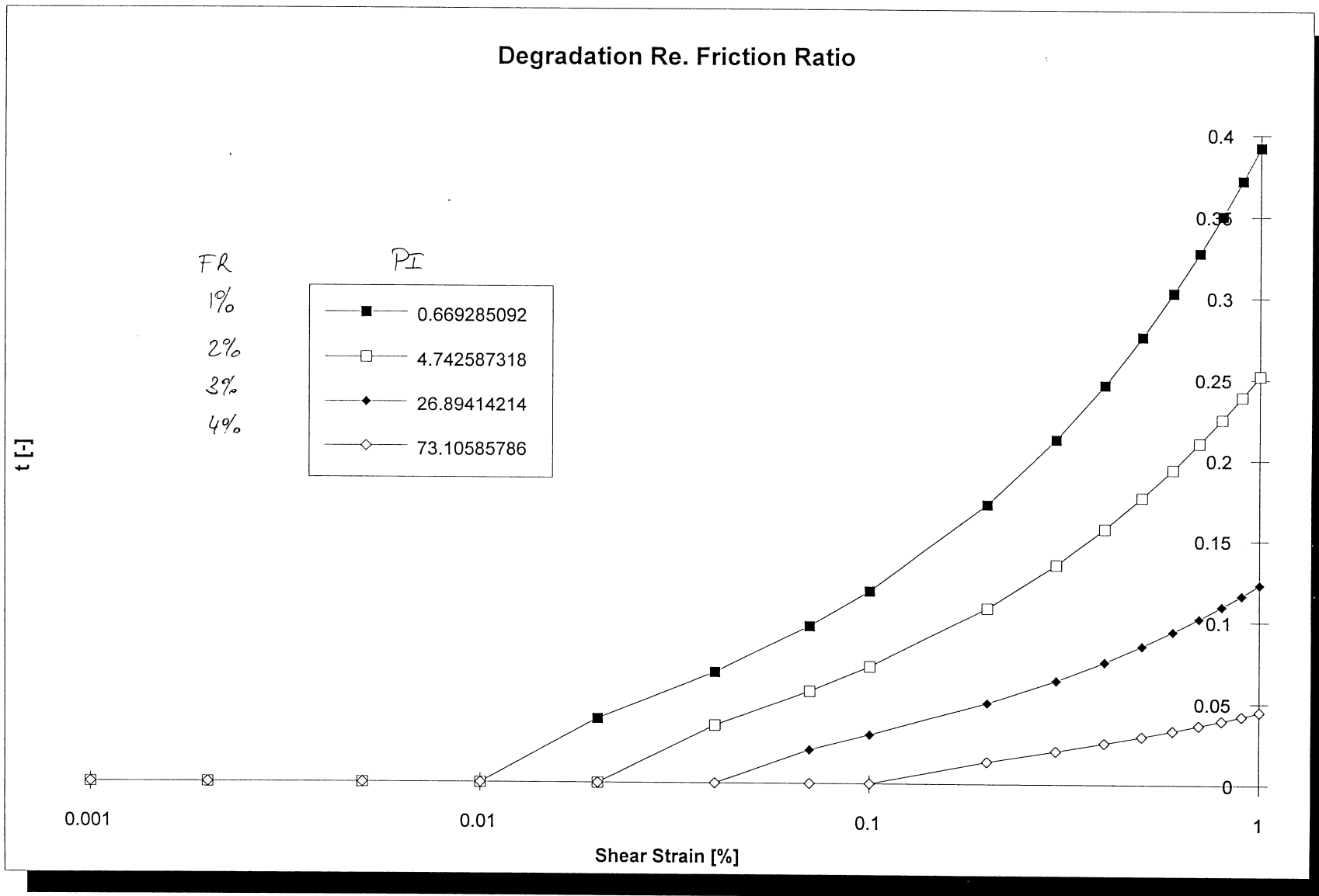


Fig. 28. Degradation Parameter - high values - Vs shear strain for different FR (Chart 6e)

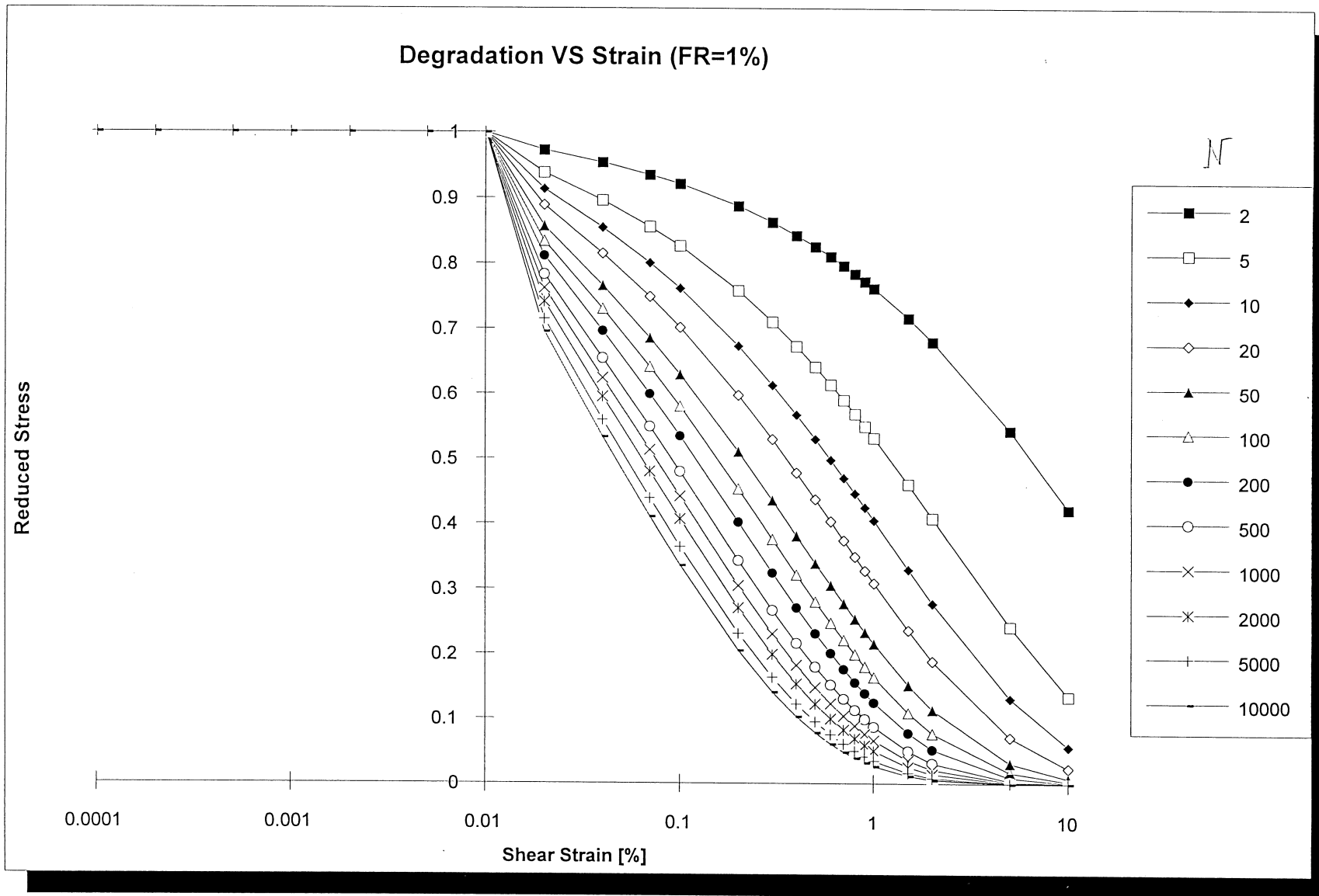


Fig. 29. Degradation Vs Strain (FR=1%) - (Chart 10a)

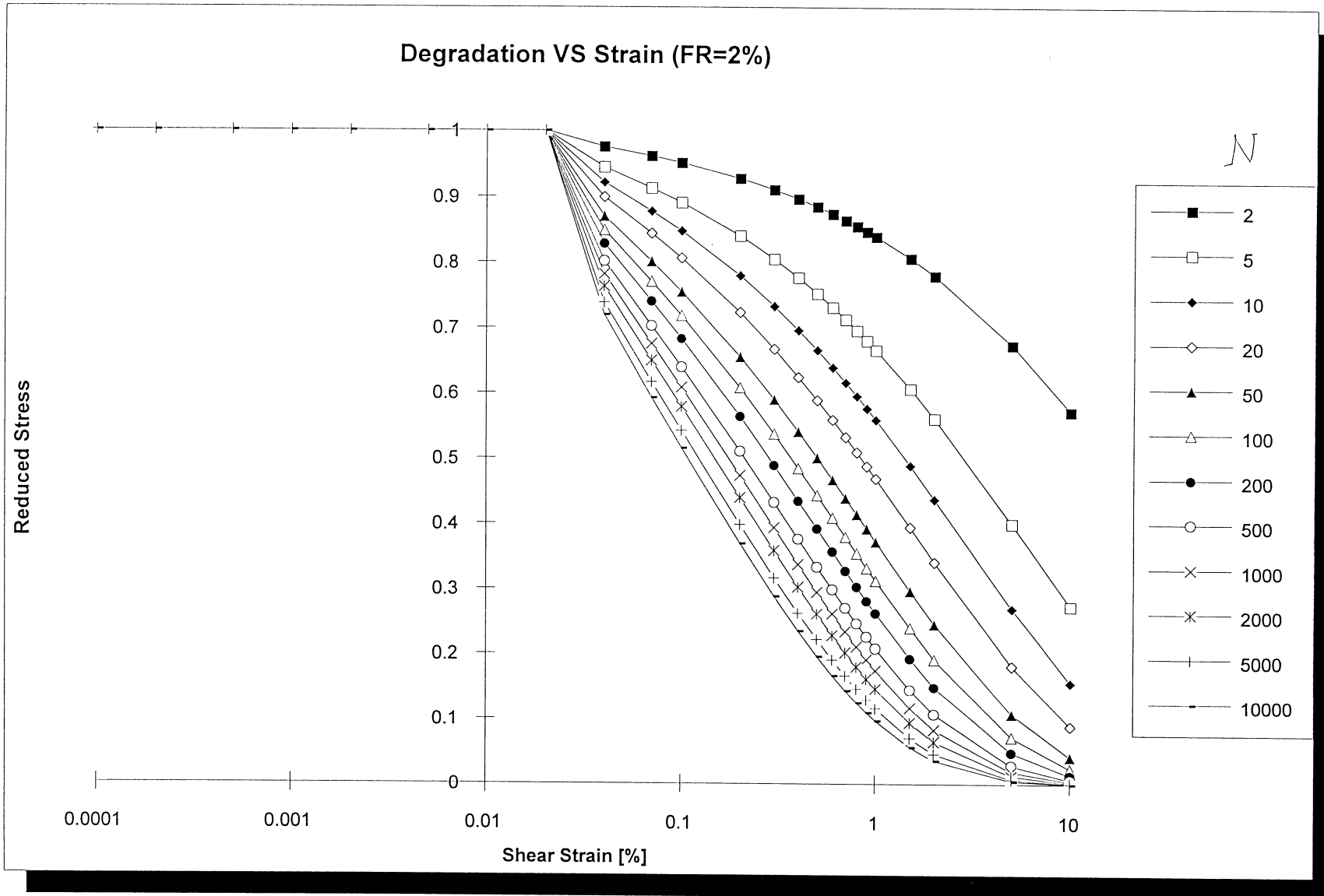


Fig. 30. Degradation Vs Strain (FR=2%) - (Chart 10b)

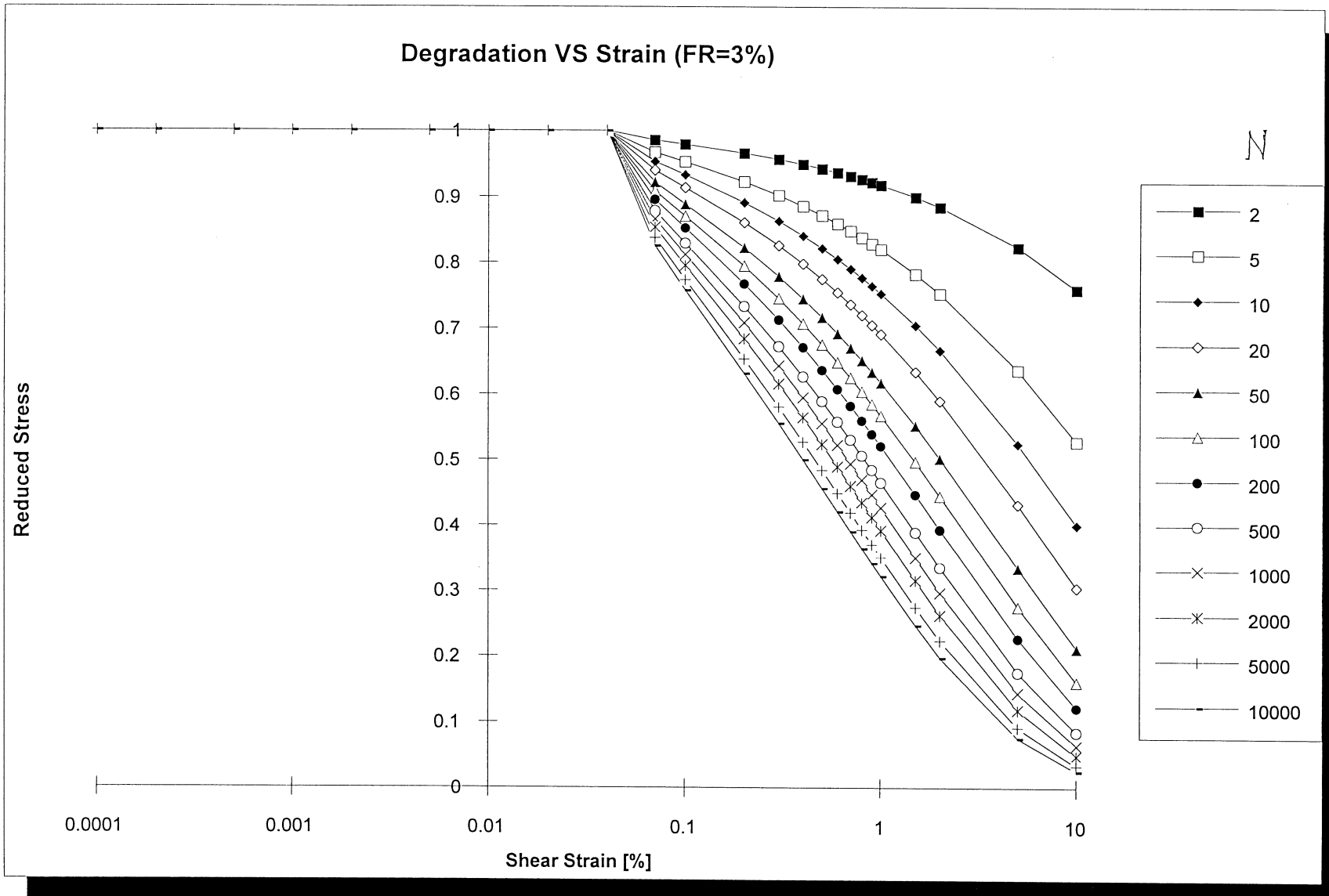


Fig. 31. Degradation Vs Strain (FR=3%) - (Chart 10c)

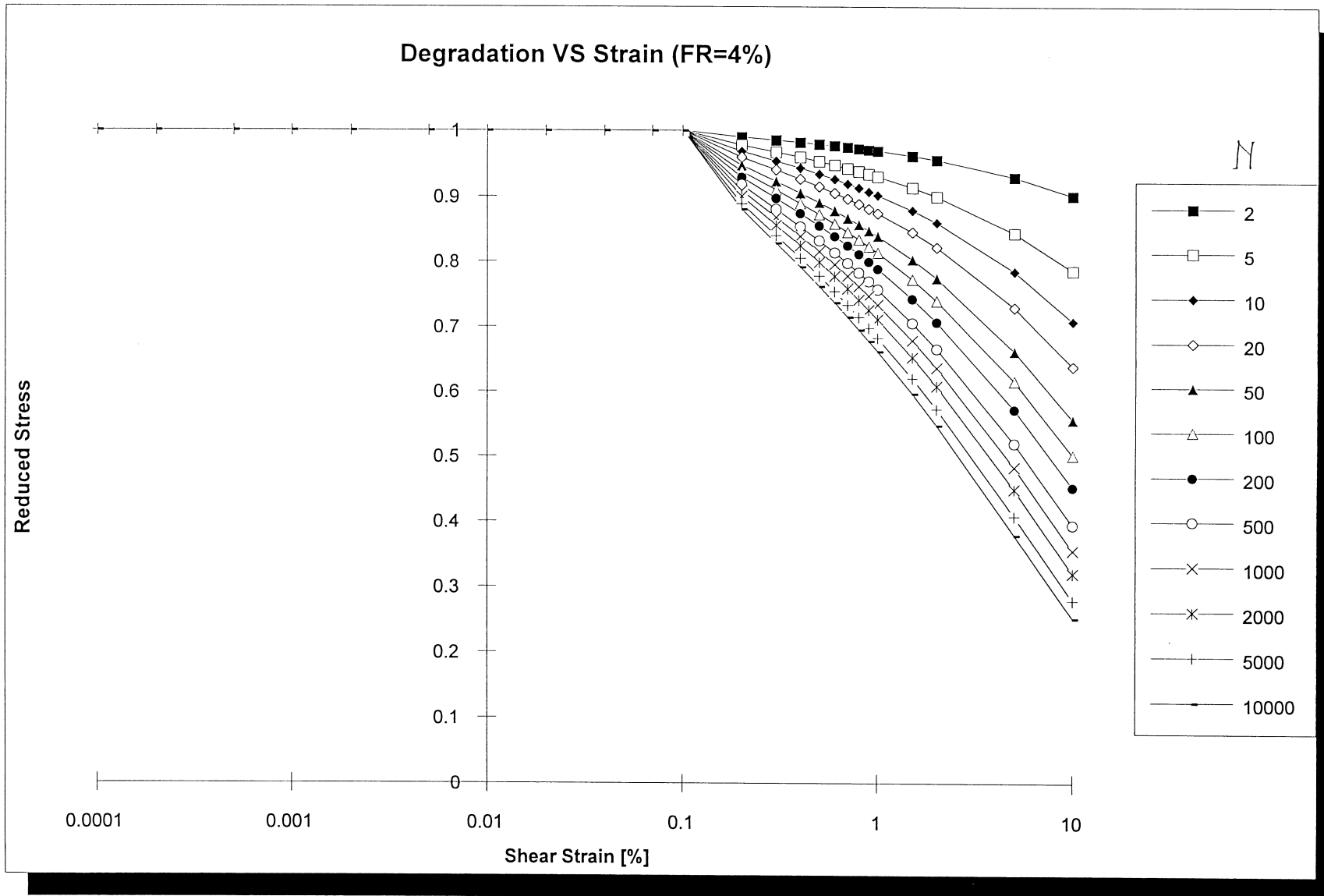


Fig. 32. Degradation Vs Strain (FR=4%) - (Chart 10d)

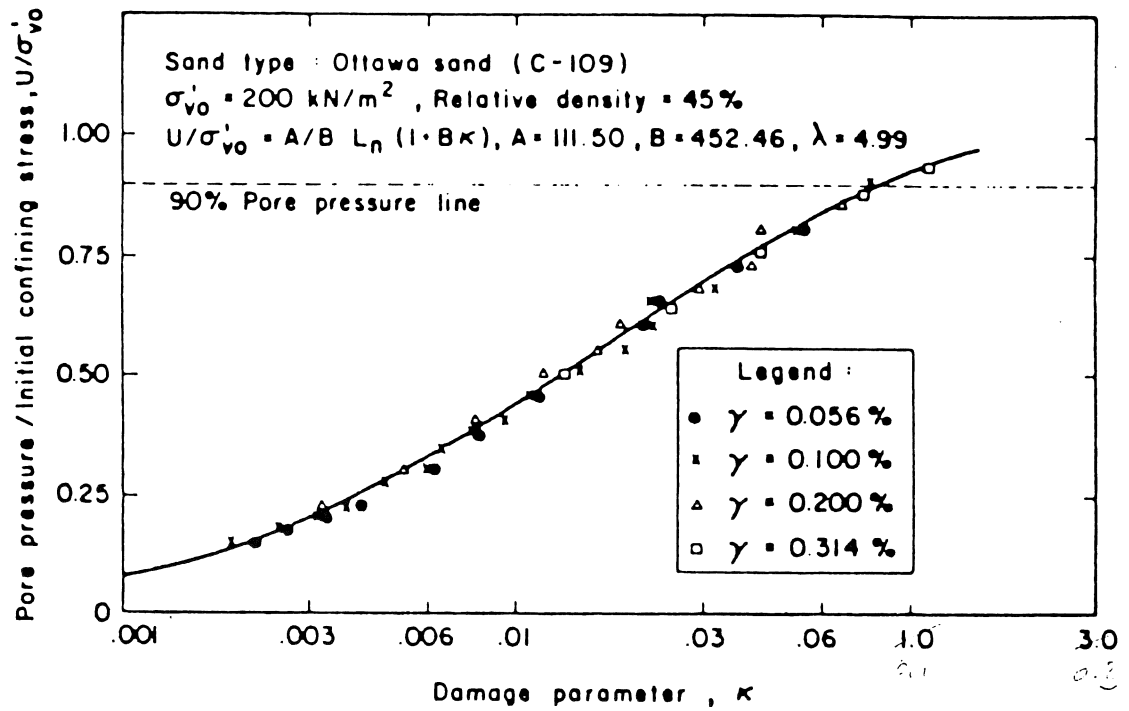


FIGURE 33 Pore pressure versus damage parameter  $k$  (logarithmic scale). Source: Finn (1981).

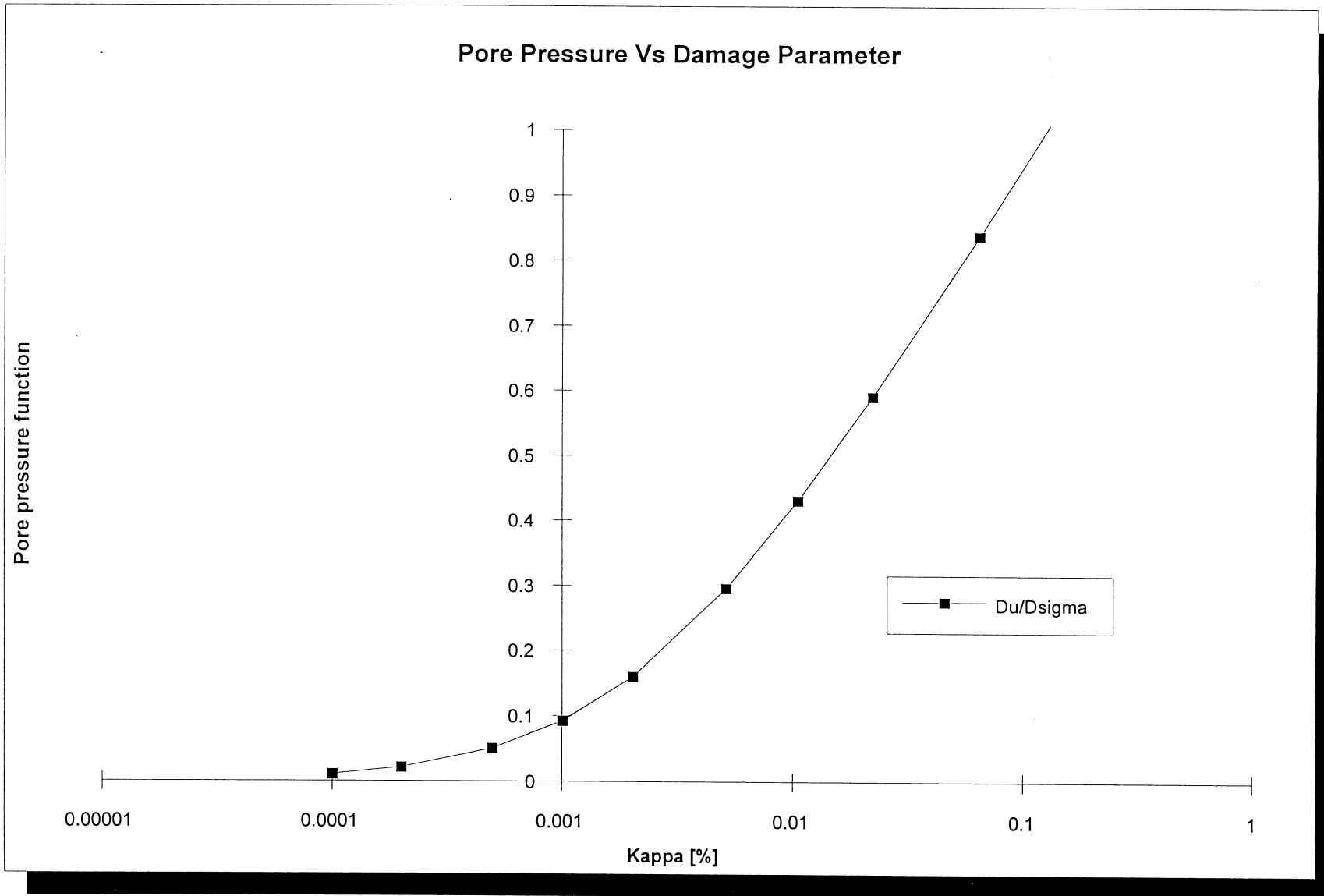


Fig. 34. Pore pressure Vs damage parameter (Chart 7)

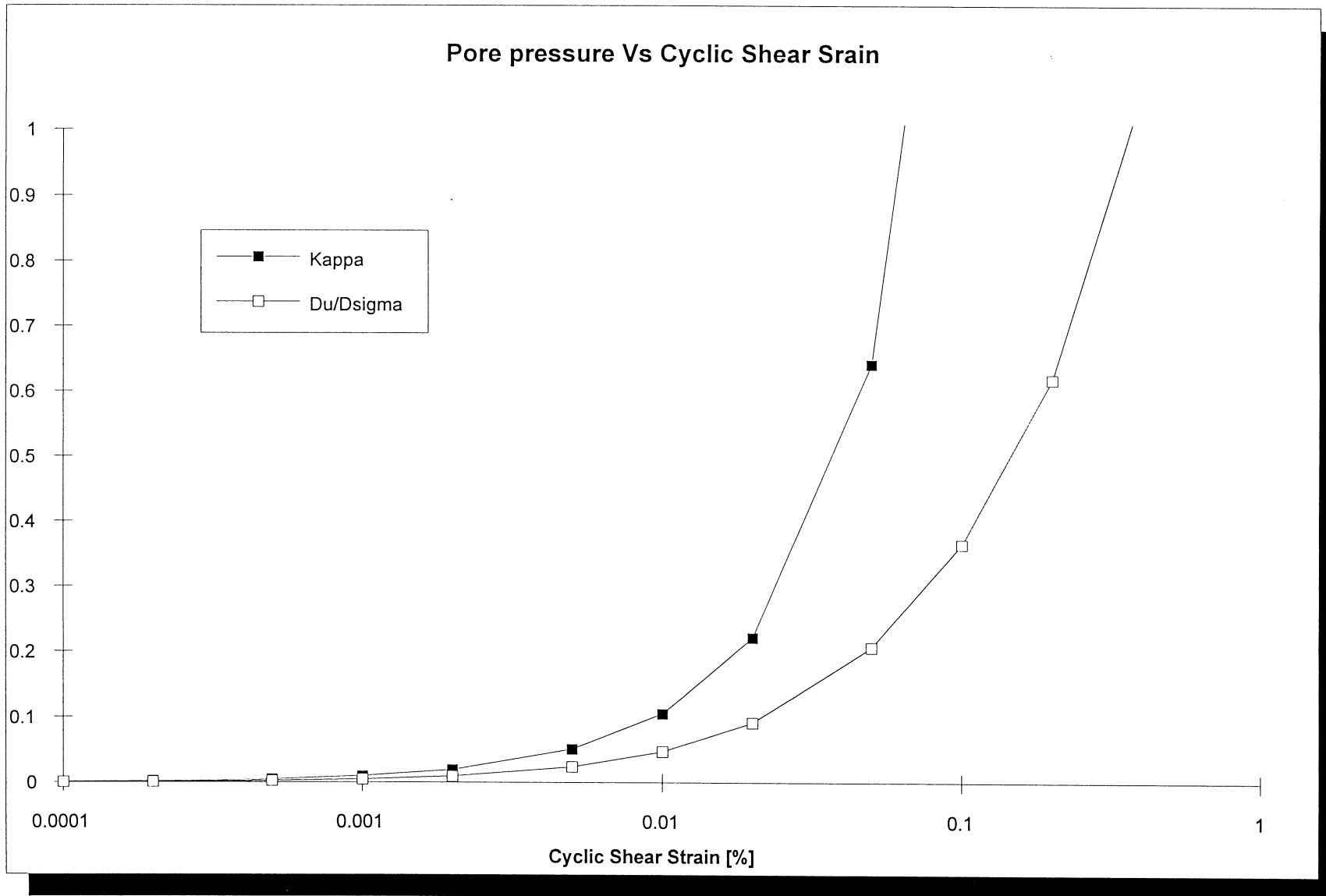


Fig. 35. Pore pressure Vs cyclic shear Strain (Chart 8)

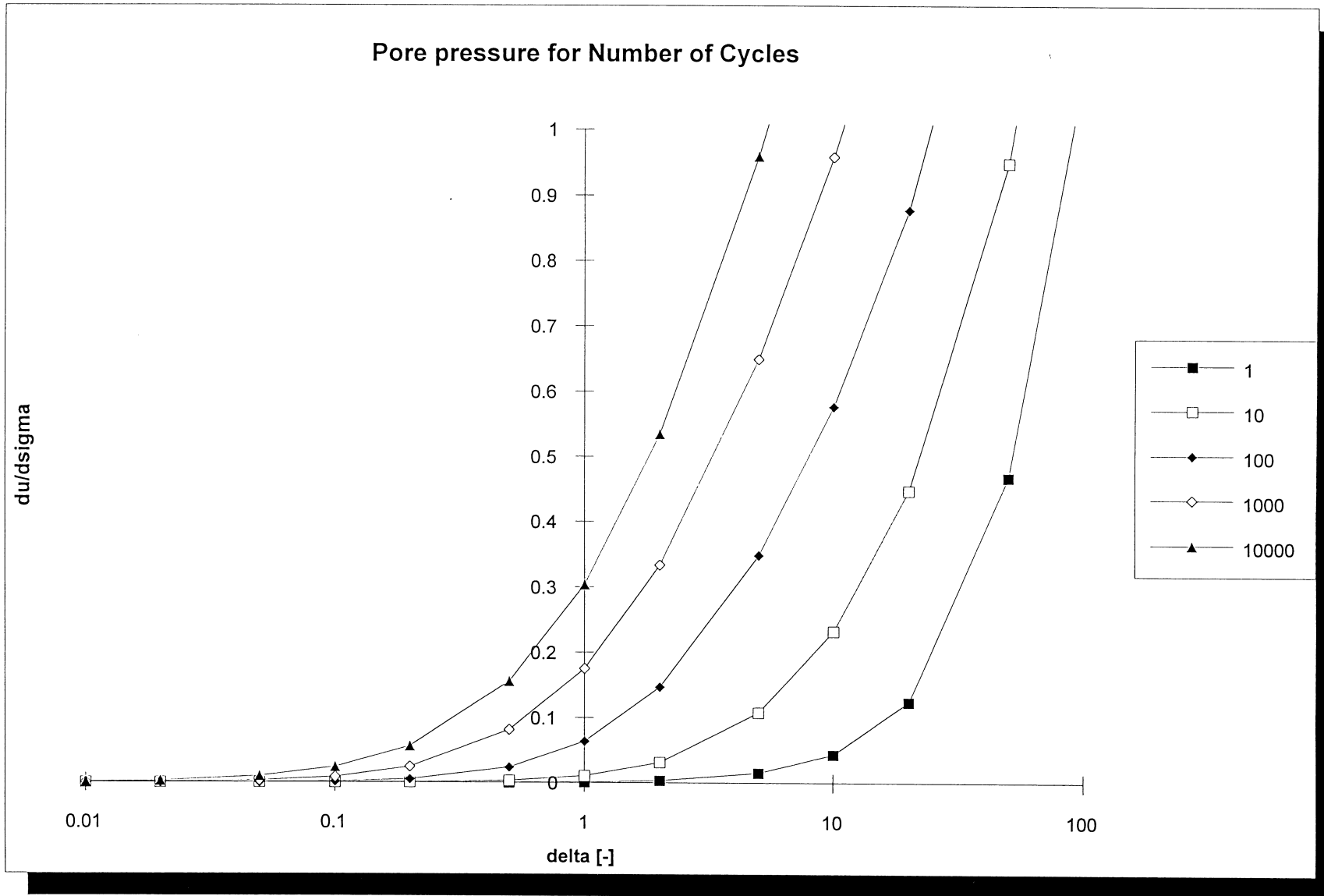


Fig. 36. Pore pressure Vs relative strain for different numbers of cycles (Chart 9)